Plant Physiology Preview. Published on May 23, 2016, as DOI:10.1104/pp.16.00670

Running head: MHPP modulates root development

Author for correspondence: Jin Xu

Key Laboratory of Tropical Plant Resources and Sustainable Use, Xishuangbanna Tropical Botanical Garden, Chinese Academy of Sciences, Menglun, Mengla, Yunnan 666303, China

Tel: 86 871 65140420

Email: xujin@xtbg.ac.cn

Research Area: Signaling and Response

The nitrification inhibitor methyl 3-(4-hydroxyphenyl)propionate modulates root development by interfering with auxin signaling via the NO/ROS pathway in *Arabidopsis*

Yangyang Liu[†], Ruling Wang[†], Ping Zhang, Qi Chen, Qiong Luo, Yiyong Zhu, and Jin Xu[*]

Key Laboratory of Tropical Plant Resources and Sustainable Use, Xishuangbanna Tropical Botanical Garden, Chinese Academy of Sciences, Menglun, Mengla, Yunnan 666303, China (Y.-Y.L., R.-L.W., P.Z., Q.L., J.X.); Faculty of Life Science and Technology, Kunming University of Science and Technology, Jingming South Road, Kunming, 650500, China (Q.C.) and College of Resources and Environmental Sciences, Nanjing Agricultural University, Nanjing, 210095, China (Y.-Y.Z.)

[†] These authors have contributed equally to this work.

One-sentence summary: MHPP affects root development via the NO/ROS-mediated auxin response pathway.

Contributions

J.X. conceived the original screening and research plans; J.X. and Y.Y.L. supervised the experiments; Y.Y.L. and R.L.W. performed most of the experiments; R.L.W., P.Z., Q.L., Q.C., and Y.Y.Z. provided technical assistance to Y.Y.L.; J.X. and Y.Y.L. designed the experiments and analyzed the data; J.X. conceived the project and wrote the article with contributions of all the authors; J.X. supervised and complemented the writing.

Footnotes:

This work was supported by China National Natural Sciences Foundation (31170228, 31272239, 31172035), the Key Project of State Key Laboratory of Desert and Oasis Ecology, Xinjiang Institute of Ecology and Geography of Chinese Academy of Sciences, Yunnan Province Foundation for academic leader (2014HB043), the Knowledge Innovation Program of the Chinese Academy of Sciences (Grant No. KSCX2-EW-Z-15), Hebei Province National Natural Sciences Foundation for Distinguished Young Scientists (C2013503042), and the Program for New Century Excellent Talents in University (NCET-11-0672).

Abstract

Methyl 3-(4-hydroxyphenyl)propionate (MHPP) is a root exudate that functions as a nitrification inhibitor and as a modulator of the root system architecture (RSA) by inhibiting primary root (PR) elongation and promoting lateral root formation. However, the mechanism underlying MHPP-mediated modulation of the RSA remains unclear. Here, we report that MHPP inhibits PR elongation in *Arabidopsis* by elevating the levels of auxin expression and signaling. MHPP induces an increase in auxin levels by up-regulating auxin biosynthesis, altering the expression of auxin carriers, and promoting the degradation of the auxin/indole-3-acetic acid family of transcriptional repressors. We found that MHPP-induced nitric oxide (NO) production promoted reactive oxygen species (ROS) accumulation in root tips. Suppressing the accumulation of NO or ROS alleviated the inhibitory effect of MHPP on PR elongation by weakening auxin responses and perception and by affecting meristematic cell division potential. Genetic analysis supported the phenotype described above. Taken together, our results indicate that MHPP modulates RSA remodeling via the NO/ROS-mediated auxin response pathway in *Arabidopsis*. Our study also revealed that MHPP significantly induced the accumulation of glucosinolates in roots, implying the diverse functions of MHPP in modulating plant growth, development, and stress tolerance in plants.

Introduction

Nitrogen fertilizer is one of the most expensive nutrients to supply (Fan et al., 2009). Nitrification results in the transformation of ammonium to nitrate via nitrite in a reaction that is mediated by ammonia-oxidizing bacteria. However, nitrogen can be lost through the leaching of nitrate and gaseous nitrogen emissions, with potential adverse effects on the environment and human health (Subbarao et al., 2013). The low efficiency of agronomic nitrogen application is largely the result of nitrogen loss associated with nitrification and denitrification (Schlesinger, 2009; Subbarao et al., 2013). High levels of nitrification can lead to nitrogen starvation, which in turn forces plants to develop strategies to reduce nitrogen loss (Subbarao et al. 2013). Some plants, such as *Brachiaria* grasses, have developed mechanisms to suppress nitrification via the exudation of specific secondary organic compounds from roots; this process is termed "biological nitrification inhibition (BNI)". Zakir et al. (2008) found that the root exudates of *Sorghum bicolor* possess BNI activity, and a subsequent study confirmed that BNI activity was attributable to multiple components present in the sorghum exudate and identified the isolated phenolic substance methyl 3-(4-hydroxyphenyl)propionate (MHPP) as the main active compound (Nardi et al., 2013). NH_4^+ induced greater MHPP production in plants (56.6 μM g^{-1} root DW d^{-1}) than standard Hoagland medium alone (17 μM g^{-1} root DW d^{-1}) (Zakir et al., 2008). Although MHPP has been demonstrated to inhibit nitrification, no further studies have been undertaken to characterize the effect of MHPP as a root exudate on plant growth and root system development.

Root system growth and development are complex processes that are modulated by a variety of phytohormones and signaling molecules, including auxin, ethylene, abscisic acid (ABA), nitric oxide (NO), and reactive oxygen species (ROS), as well as their interactions (Van de Poel et al., 2015). Auxin plays a central role in regulating root growth by positioning the stem cell niche, controlling division of the meristem, and increasing cell volume in the elongation zone via the modulation of auxin biosynthesis, transport, and responses (Wang et al., 2009). Maintaining a maximal auxin concentration in the quiescent center (QC) and a steep auxin gradient in the proximal meristem, which decreases with increasing distance from the QC, is required for normal root growth (Laskowski et al., 2008). The auxin influx carriers in the AUXIN1/LIKE AUX1 (AUX1/LAX) family and efflux carriers in the PIN-FORMED

(PIN) family mediate polar auxin transport (PAT) in plants and subsequent root system architecture (RSA) remodeling in response to environmental cues, including biotic and abiotic stresses. Different auxin carriers can modulate a common physiological process or stress response via various signaling pathways. For example, both PIN2 and AUX1 are required for plant adaptation to alkaline stress. PIN2 induces alkaline stress adaptation via a PKS5-mediated signaling cascade to modulate proton secretion in root tips to maintain primary root (PR) elongation (Xu et al., 2012; Li et al., 2015). AUX1 is involved in alkaline stress-induced RSA remodeling via ethylene-mediated auxin accumulation (Li et al., 2015). Additionally, AUX1 and PIN2 sustain lateral root (LR) formation in *Arabidopsis* during the early stages of iron (Fe) toxicity (Li et al., 2015).

NO has been identified as an important signaling molecule that interplays with ROS in response to stresses and in the regulation of root growth. NO protects plant cells against oxidative stress by reducing ROS accumulation (Wink and Mitchell, 1998; Xu et al., 2010a). The NO biosynthesis-related mutant *nitric oxide-associated1* (*noa1*) exhibits reduced PR elongation in association with increased ROS accumulation. Our previous study indicated that zinc (Zn) toxicity-induced NO accumulation increased the ROS level in *Solanum nigrum* roots by modulating the expression and activity of antioxidative enzymes and that this elevation of ROS production resulted in programmed cell death (PCD) in root tips; thus, NO modulates the RSA and the subsequent adaptation of the RSA in response to Zn stress (Xu et al., 2010a).

Synergistic effects of NO and auxin on a series of plant responses have been observed. Exogenous auxin application increased NO production (Correa-Aragunde et al., 2004; Lombardo et al., 2006), and NO accumulation in roots mediates auxin-induced LR formation (Correa-Aragunde et al., 2004), adventitious root growth (Tewari et al., 2008) and root hair development (Lombardo et al., 2006). Our previous study indicated that NO elevates the indole-3-acetic acid (IAA) level in cadmium-treated *Medicago* roots by reducing its degradation via IAA oxidase activity, thereby promoting auxin equilibrium and ameliorating cadmium toxicity (Xu et al., 2010b). Fernández-Marcos et al. (2011) found that a high NO level inhibits rootward auxin transport in *Arabidopsis* roots by reducing the abundance of PIN1. Terrile et al. (2012) found that S-nitrosylation of the auxin receptor TIR1promotes its interaction with auxin/IAA (Aux/IAA) proteins, which are transcriptional repressors of genes

associated with auxin responses. The NO biosynthesis-related triple mutant *nitrate reductase 1 (nia1)/nia2/noa1* exhibits reduced NO levels and small root meristems with abnormal divisions. Further investigation indicated that the abnormal phenotypes of this NO mutant are related to perturbations in auxin biosynthesis, transport and signaling (Sanz et al., 2014).

Similar to NO, ROS might also regulate root growth and development by modulating auxin homeostasis and signaling. The expression of auxin-responsive genes is decreased by H_2O_2 treatment via mitogen-activated protein kinase activation (Kovtun et al., 2000). Defects in antioxidative capacity caused by simultaneous thioredoxin and glutathione mutation result in altered auxin homeostasis and development (Bashandy et al., 2010). Blomster et al. (2011) found that apoplastic O_3 transiently suppressed auxin signaling by reducing the gene expression levels of auxin receptors and Auxin/indole-3-acetic acid (Aux/IAA) family transcriptional repressors. However, auxin receptor mutants are more tolerant to H_2O_2 (Iglesias et al., 2010); therefore, reducing the expression of auxin receptor genes might be an adaptive mechanism by which plants respond to ROS accumulation.

Here, we report that the MHPP, in addition to its function as a nitrification inhibitor, acts as an important regulator of the RSA by inhibiting PR elongation and promoting LR formation in *Arabidopsis* seedlings by regulating the auxin levels in the root tip and modulating meristematic cell division potential. We found that exogenous MHPP increased the levels of auxin signaling by promoting the expression of IAA biosynthesis-related genes, increasing auxin perception via the destabilization of Aux/IAA, and significantly repressing the expression of PIN4 in root tips. Furthermore, MHPP-induced NO production promoted an increase in ROS accumulation in root tips, and inhibition of NO/ROS accumulation ameliorated the MHPP-induced reduction in PR growth. Genetic analysis supported the phenotype described above. Our study also revealed that MHPP significantly induced the accumulation of glucosinolates in roots. The potential mechanisms involved in this process are discussed.

164

Results

Effects of MHPP on Primary Root Development

Previous studies indicated that the root exudate MHPP exerts a significant inhibitory effect on nitrification in soil. To further explore whether MHPP could modulate root system development, five-day-old *Arabidopsis* seedlings germinated on half-strength MS (1/2 MS) plates were transferred to new plates supplemented with or without 40 or 80 μM MHPP for continued growth for 5 d, and the PR growth and LR number were measured. PR elongation was inhibited and LR number was increased in the presence of either 40 or 80 μM MHPP, and these effects were positively associated with the MHPP concentration (Fig. 1A, 1B, and 1F). Specifically, PR elongation was inhibited by 25% and 46% in seedlings exposed to 40 μM and 80 μM MHPP, respectively (Fig. 1B). The LR number was increased by 158% and 205% following exposure to 40 μM and 80 μM MHPP, respectively (Fig. 1F). To further explore the effect of MHPP on LR formation, we analyzed lateral root primordium (LRP) initiation. As shown in Fig. 1G, LRP initiation was enhanced in all four stages following exposure to 40 μM or 80 μM MHPP. To examine the inhibitory effects of MHPP on PR elongation in detail, we also measured the lengths of meristem zones and elongation zones in the MHPP-treated roots. As shown in Fig. 1C and 1D, the lengths of both meristem zones and elongation zones were decreased in the roots exposed to 40 μM or 80 μM MHPP. MHPP treatment also reduced the average cell length in the differentiation zone (Fig. 1E).

PR growth inhibition can be caused by reductions in stem cell niche activity and meristematic cell division potential in root tips (Baluska et al., 2010; Li et al., 2015). Therefore, we first analyzed the possible change in stem cell activity using the QC-specific marker *QC25:GUS* (Sabatini et al., 1999). GUS staining in the QC showed a similar expression pattern between control- and MHPP-treated roots (Supplemental Fig. S1A and 1D). *PLETHORA* (*PLT*) acts in concert with *SHORT ROOT* (*SHR*) to control QC identity (Sabatini et al., 2003). Thus, we next analyzed the influence of MHPP on the expression of PLT1 and SHR. Examination of *PLT1pro:PLT1-GFP* and *SHRproSHR-GFP* activities indicated that the expression levels of both the PLT1 and SHR reporters were unaltered in MHPP-treated roots compared with the control-treated roots (Supplemental Fig. S1B, S1C, S1E, and S1F).

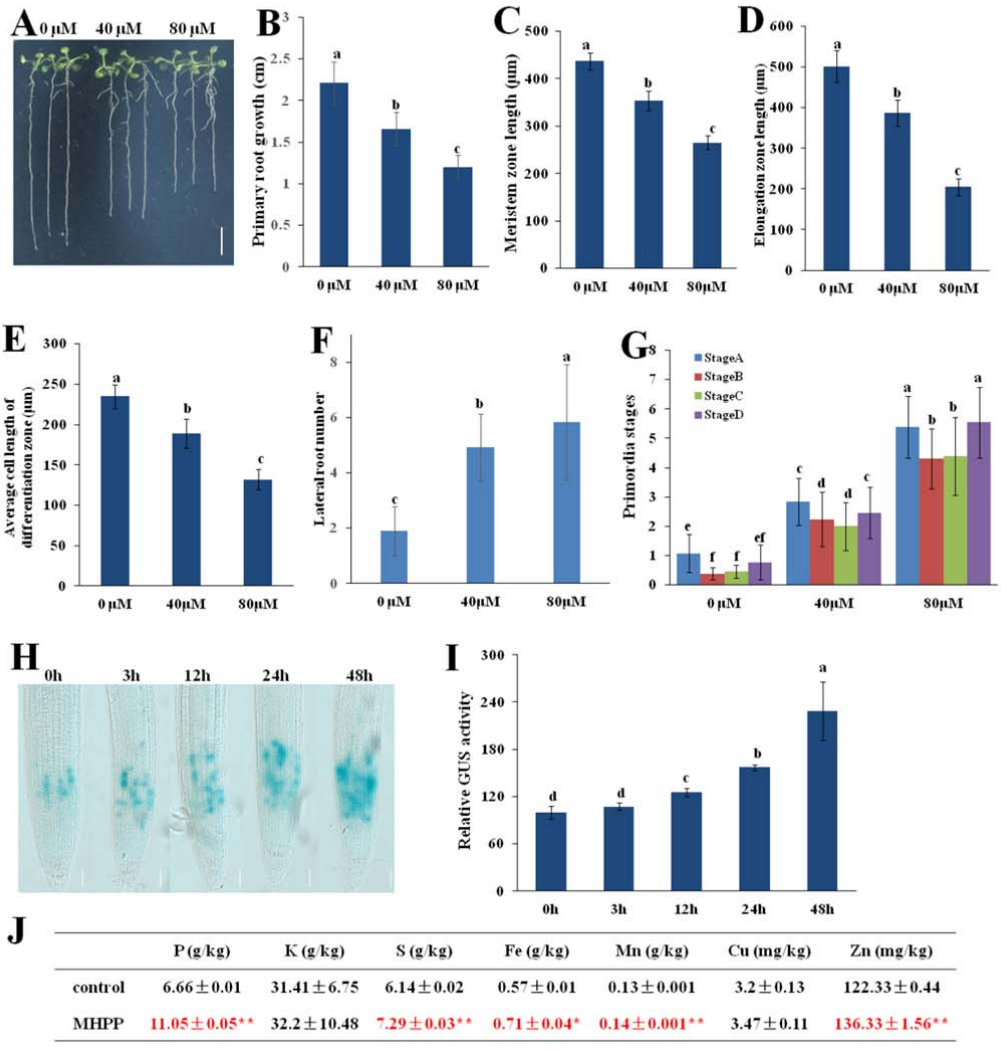

J

	P (g/kg)	K (g/kg)	S (g/kg)	Fe (g/kg)	Mn (g/kg)	Cu (mg/kg)	Zn (mg/kg)
control	6.66±0.01	31.41±6.75	6.14±0.02	0.57±0.01	0.13±0.001	3.2±0.13	122.33±0.44
MHPP	11.05±0.05**	32.2±10.48	7.29±0.03**	0.71±0.04*	0.14±0.001**	3.47±0.11	136.33±1.56**

Fig.1 MHPP affected root system development in *Arabidopsis*. (A-G) Five-day-old wild-type seedlings grown in 1/2 MS medium were treated with 40 or 80 μM MHPP for 5 d (A). Bar, 0.5 cm. Primary root elongation (B), the lengths of meristem zones (C) and elongation zones (D), the average cell length in the differentiation zone (E), the number of lateral roots (F), and lateral root primordium initiation (G) were measured after 5 d of treatment. (H,I) Image of GUS staining in 5-d-old *CYCB1;1:GUS* seedlings exposed to 40 μM MHPP for 3-48 h (H) and the relative GUS activity of *CYCB1;1:GUS* seedlings (I) treated as in (H). Bars, 50 μm. The level of GUS activity in untreated roots was set to 100. The error bars represent the SEM. Different letters indicate significantly different values ($P < 0.05$ by Tukey's test). (J) Nutrient element contents in MHPP-treated *Arabidopsis* seedlings. The ± symbol represents the SEM. The asterisks indicate significant differences with respect to the corresponding control based on Tukey's test (*, $0.01<P<0.05$; **, $P<0.01$).

We next examined meristematic cell division potential in a transgenic line expressing *CYCB1;1:GUS*, a marker used to monitor cell cycle progression (Colon-Carmona et al., 1999). Histochemical staining showed that GUS activity was dramatically higher in MHPP-treated roots than in control-treated roots (Fig. 1H and 1I, Supplemental Fig. S1G). It is known that *CYCB1;1* transcription is activated during G2 phase and that CYCB1;1 is degraded at metaphase (Zheng et al., 2011). The increased accumulation of CYCB1;1 suggests that cell cycle progression was hampered at the G2 to M phase

transition. These data indicated that MHPP inhibited PR growth by affecting meristematic cell division potential.

The above results show that MHPP inhibited PR elongation while increasing LR number, thereby modulating the RSA. The root system is the major organ through which plants absorb nutrient elements. Thus, we examined the nutrient element contents in seedlings. ICP-MS analysis indicated that MHPP treatment markedly increased the contents of phosphorus (P), sulfur (S), Fe, manganese (Mn) and Zn and slightly increased the potassium (K) and copper (Cu) contents in seedlings (Fig. 1J). These data indicated that MHPP improved nutrient element accumulation in plants.

Auxin Is Involved in the MHPP-Mediated Inhibition of Primary Root Meristem Development

Auxin plays an essential role in root system development and root meristem maintenance (Overvoorde et al., 2010). The altered RSA and root meristem patterning observed in MHPP-treated seedling raised the question of whether the auxin content is affected by MHPP. Therefore, we measured the IAA level in MHPP-treated roots using gas chromatography/mass spectrometry (GC/MS) and found that the IAA level was higher in MHPP-treated roots than in control-treated roots (Fig. 2A). We then tested the hypothesis that MHPP affects auxin signaling in the root apical meristem (RAM). For this purpose, we used seedlings expressing the auxin-responsive marker *DR5:GFP*. Seedlings were grown on 1/2 MS medium for 5 d, followed by treatment with or without 40 or 80 μM MHPP for up to 24 h, during which GFP fluorescence was monitored. MHPP indeed increased the expression of the auxin reporter in root tips until 12 h, but the expression of this reporter returned to the control level after 24 h of treatment (Fig. 2B and 2C; Supplemental Fig. S2A and S2B).

To investigate how MHPP increased the auxin levels, we conducted quantitative reverse transcription-polymerase chain reaction (qRT-PCR) analysis to estimate the transcript levels of the genes that encode for key enzymes in the auxin biosynthesis pathway. Consistent with the finding of increased IAA levels in roots, the qRT-PCR results revealed that MHPP significantly increased the transcript levels of many IAA biosynthesis genes, including *ASA1*, *PAT1*, *AMI1, SUR1*, *TAA1*, *YUC2*, *YUC3*, *YUC9*,

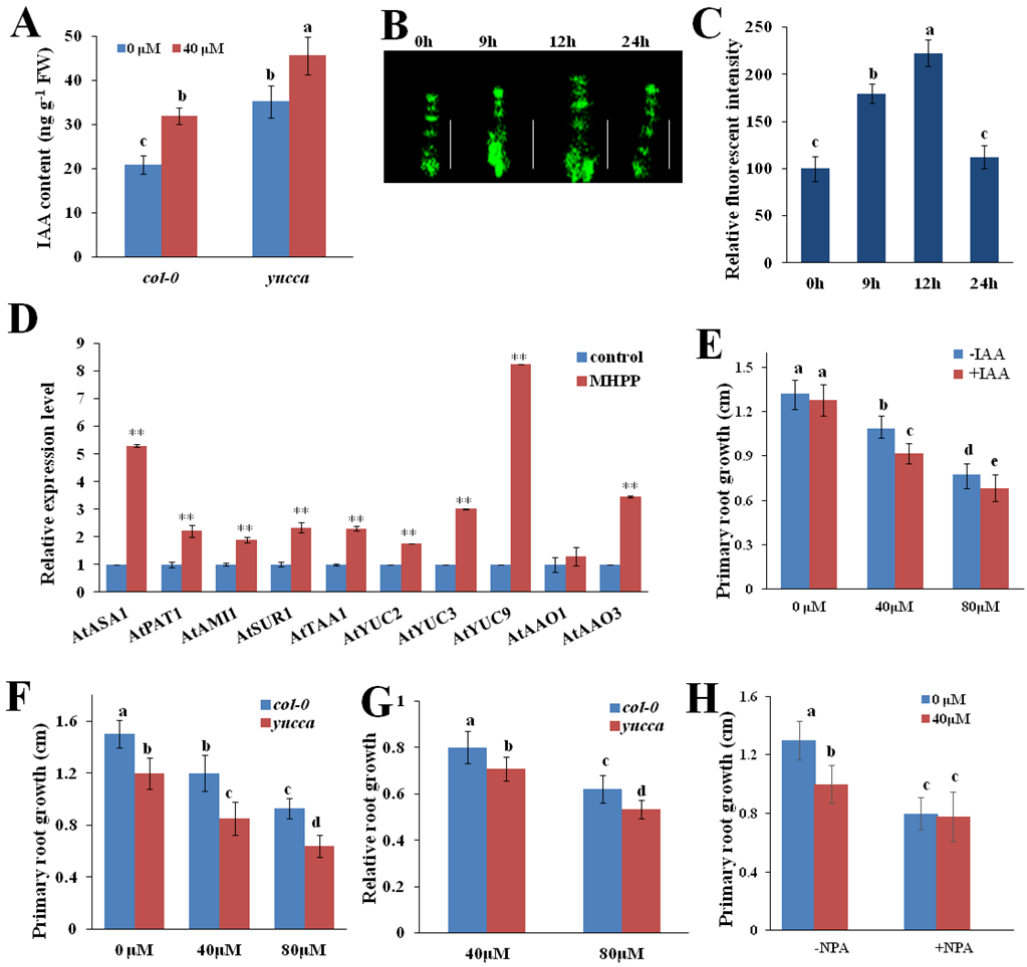

Fig. 2 MHPP treatment enhanced auxin accumulation in roots, thus inhibiting primary root growth. (A) IAA contents in the roots of *col-0* seedlings and *yucca* seedlings treated with or without 40 μM MHPP for 24 h. (B,C) GFP fluorescence in the roots of 5-d-old *DR5:GFP* seedlings exposed to 40 μM MHPP for 9-24 h (B) and quantification of *DR5:GFP* fluorescence intensity (C) in plants treated as in (B). The fluorescence intensity of untreated roots was set to 100. Bars, 50 μm. (D) Quantitative real-time reverse transcription-polymerase chain reaction (qRT-PCR) analysis of the gene expression of auxin biosynthesis-related genes in *col-0* seedlings treated with or without 40 μM MHPP for 12 h. The expression levels of the indicated genes in untreated roots were set to 1. (E) Primary root growth of *col-0* seedlings treated with or without MHPP (40 μM or 80 μM) in the presence of 0 or 0.5 nM IAA for 2 d. (F, G) Primary root growth of *col-0* seedlings and *yucca* seedlings treated with or without MHPP (40 μM or 80 μM) for 2 d (F) and the relative root growth of seedlings of the two genotypes treated with 40 μM or 80 μM MHPP compared with untreated seedlings (G). (H) Primary root growth of wild-type seedlings treated with or without 40 μM MHPP in the presence or absence of 1 μM NPA for 2 d. The error bars represent the SEM. The asterisks (**) indicate significant differences with respect to the corresponding control (P<0.01 based on Tukey's test). Different letters indicate significantly different values (P < 0.05 by Tukey's test).

AAO1, and *AAO3* in *Arabidopsis* seedlings (Fig. 2D). These results suggest that MHPP up-regulates IAA biosynthesis gene expression, which influences the auxin content in roots, and that an increased auxin level may be responsible for the reduction in PR growth in MHPP-treated seedlings. We tested this hypothesis by exogenously applying auxin. Five-day-old seedlings germinated in 1/2 MS medium were transferred to fresh 1/2 MS medium containing 40 or 80 μM MHPP supplemented with 0.5 nM IAA, and PR elongation was measured 2 d after transfer.

As shown in Fig. 2E, application of IAA further repressed PR growth in seedlings subjected to MHPP treatment. To confirm that elevated IAA expression is involved in the MHPP-induced inhibition of PR growth, we analyzed the root growth of *yucca*, an auxin over-producing mutant (Zhao et al., 2001), during MHPP treatment. The *yucca* mutant seedlings accumulated higher IAA levels in roots (Fig. 2A) and exhibited much shorter PR elongation than wild-type (WT) seedlings (Fig. 2F and 2G). These data indicated that MHPP inhibited PR elongation by increasing auxin accumulation via increased expression of auxin biosynthesis-related genes.

PAT plays a role in auxin accumulation and distribution in root tips. The MHPP-induced changes in the auxin levels in root tips may result from changes in PAT. We thus examined the effects of naphthylphthalamic acid (NPA), an auxin transport inhibitor, on the MHPP-induced inhibition of PR elongation. Although MHPP treatment alone decreased PR growth, PR elongation was not further reduced by the addition of NPA (Fig. 2H). This result suggests that PAT is responsible for the modulation of PR growth in MHPP-treated seedlings.

PIN4 is Required for the MHPP-Induced Inhibition of Primary Root Growth

The above results show that PAT is required for the MHPP-induced inhibition of PR growth. PAT is mediated by auxin influx carriers in the AUX/LAX family and efflux carriers in the PIN family (Peret et al., 2012; Yuan et al., 2014, 2016). Thus, we examined whether MHPP treatment also affects the expression of auxin carriers in roots. We first analyzed the gene expression levels of *AUX1*, *PIN1*, *PIN2*, *PIN4*, and *PIN7* in MHPP-treated roots. As shown in Fig. 3A, MHPP treatment significantly reduced the expression levels of *PIN4* and slightly reduced the expression of *PIN1* and *PIN2* compared to the control treatment, whereas the gene expression levels of *AUX1* and *PIN7* were nearly unaffected. We then analyzed the expression levels of AUX1, PIN1, PIN2, PIN4, and PIN7 proteins in MHPP-treated roots using transgenic lines expressing *AUX1:YFP*, *PIN1:GFP*, *PIN2:GFP*, *PIN4:GFP*, or *PIN7:GFP*. As visualized by YFP or GFP fluorescence, following exposure to MHPP, the expression level of PIN4:GFP was markedly reduced. However, there were no visible differences in the changes in the cell type/tissue expression pattern of PIN4:GFP or in its membrane localization between MHPP and control treatment (Fig. 3B, 3C;

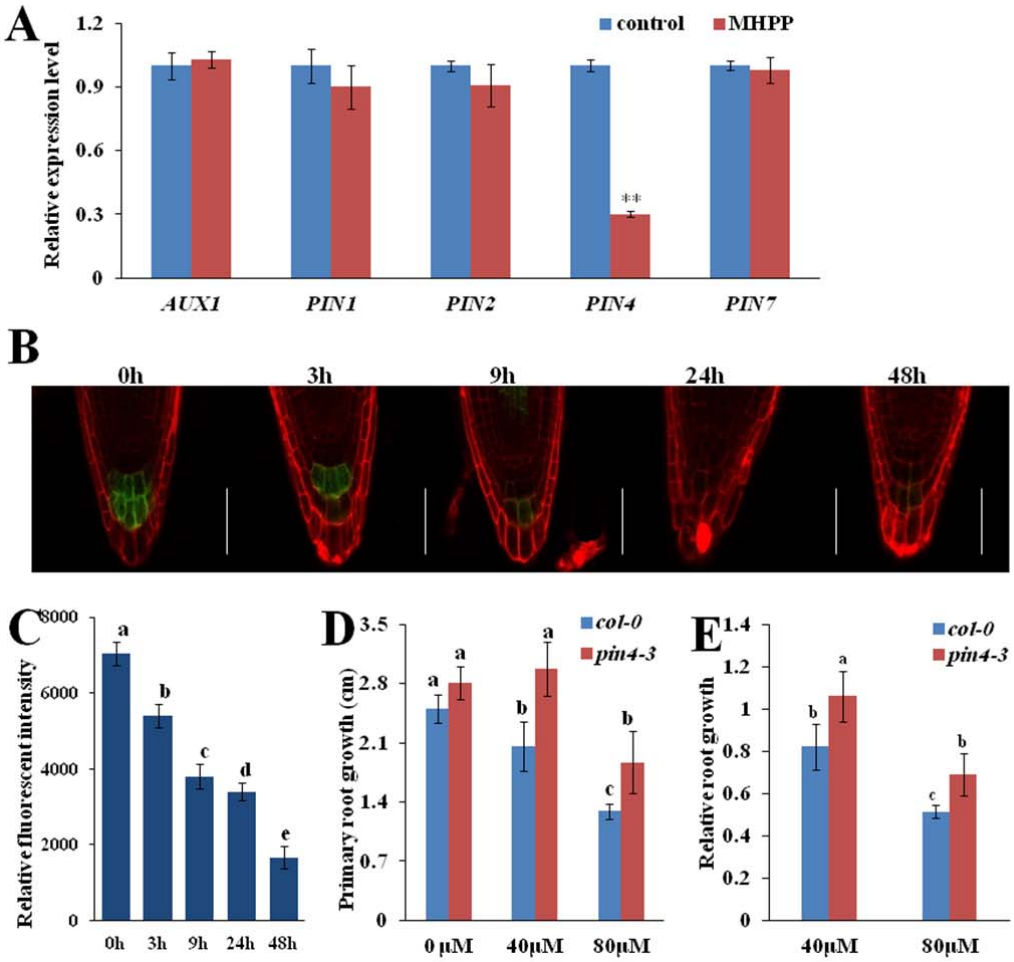

Fig. 3 PIN4 plays a role in the MHPP-mediated inhibition of primary root growth. (A) Quantitative real-time reverse transcription-polymerase chain reaction (qRT-PCR) analysis of the gene expression of auxin carrier genes in the roots of *col-0* seedlings treated with or without 40 μM MHPP for 12 h. The expression levels of the indicated genes in untreated roots were set to 1. (B,C) GFP fluorescence in the roots of 5-d-old *PIN4:GFP* seedlings exposed to 40 μM MHPP for 3-48 h (B) and quantification of the *PIN4:GFP* fluorescence intensity (C) in plants treated as in (B). Bars, 50 μm. (D, E) Primary root growth of *col-0* and *pin4-3* seedlings treated with or without MHPP (40 μM or 80 μM) for 2 d (D) and the relative root growth of seedlings of the two genotypes treated with 40 μM or 80 μM MHPP compared with untreated seedlings (E). The error bars represent the SEM. The asterisks (**) indicate significant differences with respect to the corresponding control ($P<0.01$ based on Tukey's test). Different letters indicate significantly different values ($P < 0.05$ by Tukey's test).

Supplemental Fig. S2C, S2D). However, the expression levels of AUX1, PIN1, PIN2, and PIN7 were unaffected (Supplemental Fig. S3). These results suggest that PIN4 is involved in the MHPP-induced changes in auxin accumulation and distribution in root tips.

We next investigated the roles of these auxin carriers in the MHPP-induced inhibition of PR growth using *aux1* and *pin* mutants. Whereas *aux1-21*, *pin1*, *pin2*, and *pin7-2* seedlings exhibited similar phenotypes to WT seedlings (Supplemental Fig. S4), *pin4-3* seedlings exhibited a less extensive reduction in PR elongation in response to MHPP treatment (Fig. 3D and 3E). These results suggest that the MHPP-mediated inhibition of PR elongation via the regulation of auxin distribution is predominantly modulated by PIN4.

MHPP Enhances Auxin Perception by Destabilizing Aux/IAA

The above results show that MHPP increased auxin distribution in root tips. To determine whether the effects of MHPP on the DR5:GFP signal involve auxin perception changes, we examined the effects of α-(p-chlorophenoxy)isobutyric acid (PCIB), which inhibits auxin signaling by stabilizing native Aux/IAA proteins (Oono et al., 2003), on the MHPP-induced inhibition of PR elongation. Although MHPP treatment alone decreased PR growth, PR elongation was not further reduced by the addition of PCIB (Fig. 4A). These results suggest that Aux/IAA proteins are responsible for the modulation of PR growth in MHPP-treated seedlings.

We next used a transgenic line expressing the VENUS protein fused to Aux/IAA-auxin interaction domain II (*DII-VENUS*) (Brunoud et al., 2012). In this transgenic line, the VENUS signal is sensitive to auxin in a dose-dependent manner, without disrupting the activity of the auxin response machinery (Brunoud et al., 2012). Five-day-old *DII-VENUS* seedlings were treated with MHPP, and YFP fluorescence was monitored. Treatment with MHPP resulted in rapid degradation of the nuclear DII-VENUS fluorescent signal but did not alter the expression of the auxin-insensitive reporter *mDII-VENUS* (Fig. 4B and 4D; Supplemental Fig. S5). These results suggest that MHPP enhances IAA perception in root tips. To confirm the effect of MHPP on

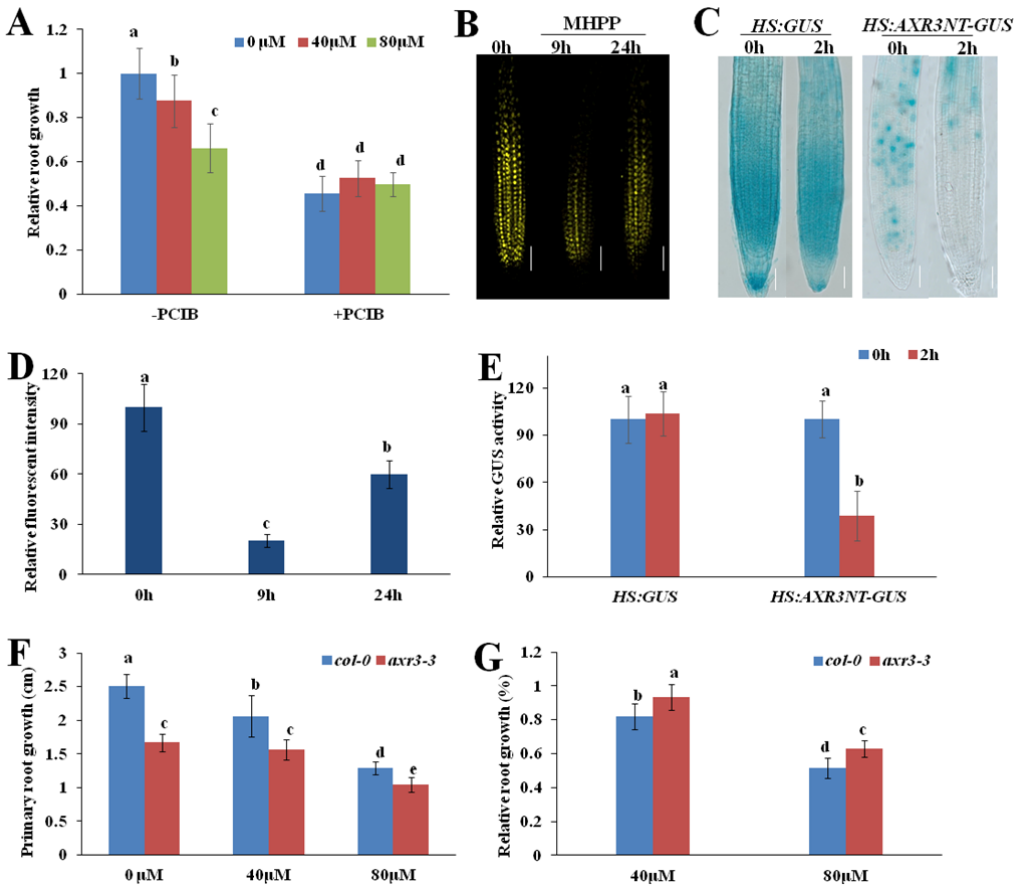

Fig. 4 MHPP treatment reduces the stability of Aux/IAA proteins. (A) Relative root growth of wild-type seedlings treated with MHPP (40 µM or 80 µM) in the presence or absence of 100 µM PCIB for 2 d. The length of untreated roots of *col-0* plants was set to 1. (B,D) YFP fluorescence in the roots of 5-d-old *DII-VENUS* seedlings exposed to 40 µM MHPP for 9 or 24 h (B) and quantification of the *DII-VENUS* fluorescence intensity (D) in plants treated as in (B). Bars, 50 µm. The fluorescence intensity of untreated roots was set to 100. (C) Image of GUS staining of 5-d-old *HS:AXR3NT-GUS* seedlings. The seedlings were heat-shocked at 37° C for 2 h and then treated with or without 40 µM MHPP for 45 min at 23° C, followed by GUS staining. Bars, 50 µm. (E) The relative GUS activity of *HS:AXR3NT-GUS* seedlings treated as in (C). The level of GUS activity in untreated roots was set to 100. (F,G) Primary root growth of *col-0* and *axr3-3* seedlings treated with or without MHPP (40 µM or 80 µM) for 2 d (F) and the relative root growth of seedlings of the two genotypes treated with 40 µM or 80 µM MHPP compared with untreated seedlings (G). The error bars represent the SEM. Different letters indicate significantly different values ($P < 0.05$ by Tukey's test).

Aux/IAA degradation, we used the *HS:AXR3-GUS* reporter line, which harbors a construct encoding for the amino terminus of the Aux/IAA protein AXR3/IAA17 and the GUS reporter under the control of a heat shock-inducible promoter (Gray et al., 2001). After heat shock, the AXR3-GUS signal significantly decreased in MHPP-treated seedlings (Fig. 4C and 4E). We therefore hypothesize that MHPP up-regulates the auxin-signaling pathway upstream of the ubiquitin-mediated degradation of Aux/IAA proteins.

To verify that Aux/IAA proteins are involved in the MHPP-induced inhibition of PR growth, we analyzed PR elongation in gain-of-function *axr3-3* mutant seedling upon

MHPP treatment (Rouse et al., 1998). The mutant seedlings exhibited less extensive suppression of PR growth in the presence of MHPP than control seedlings (Fig. 4F and 4G). These results indicate that MHPP treatment inhibits PR growth by amplifying auxin signaling in root tips by destabilizing Aux/IAA proteins.

Involvement of NO and ROS in the MHPP-Mediated Inhibition of Primary Root Growth

To assess the correlation between NO/ROS accumulation and MHPP treatment, we measured the NO and ROS levels in MHPP-treated seedlings. To visualize NO and ROS localization in roots, we used a NO-specific fluorescent probe, 4,5-diaminofluorescein diacetate (DAF-2 DA) and a ROS-specific fluorescent probe, 2,7-dichlorofluorescin diacetate (DCFH-DA). MHPP treatment induced a marked increase in NO and ROS marker fluorescence intensity from the meristem zone to the elongation zone of roots (Fig. 5A and 5B; for representative images, see Supplemental Fig. S6A and S6B, respectively). Supplementation with the NO scavenger cPTIO or the NO synthase (NOS) inhibitor L-NAME markedly inhibited the production of ROS in roots compared with MHPP treatment alone (Supplemental Fig. S7A and S7B). In contrast, supplementation with the ROS scavenger potassium iodide (KI) did not alter the NO levels in MHPP-treated roots (Supplemental Fig. S7C and S7D). To confirm that MHPP-induced NO production increases the ROS levels, we analyzed the ROS levels in *noa1*, a NO-deficient mutant, upon MHPP treatment. MHPP-induced NO accumulation was markedly reduced in *noa1* mutant roots compared with *col-0* roots (Fig. 5C and 5D). Similarly, both the ROS fluorescence and DAB staining analysis indicated that MHPP-induced ROS accumulation was also markedly reduced in *noa1* mutant roots compared with *col-0* roots (Fig. 5E and 5F; Supplemental Fig. S8). These data suggest that MHPP induces NO production upstream of ROS accumulation in roots.

To investigate the physiological mechanisms underlying the roles of NO in MHPP-mediated PR growth inhibition, 5-d-old seedlings were treated with 40 or 80 μM MHPP in the presence or absence of SNP, cPTIO or L-NAME. As shown in Fig. 6A-6F, in the presence of the NO donor SNP, the PRs of seedlings were shorter, whereas in the presence of cPTIO or L-NAME, the PRs of seedlings were longer than those of

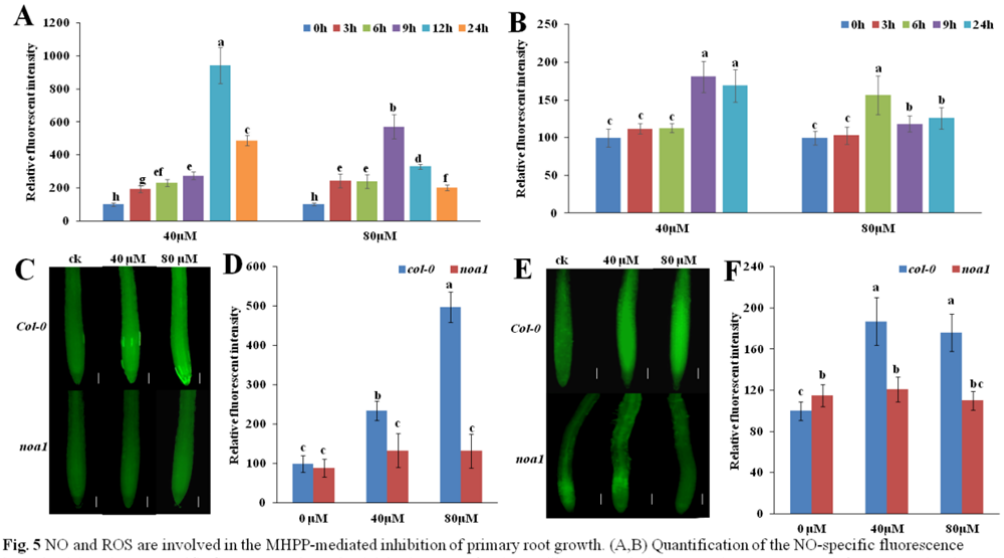

Fig. 5 NO and ROS are involved in the MHPP-mediated inhibition of primary root growth. (A,B) Quantification of the NO-specific fluorescence intensity (A) and ROS-specific fluorescence intensity (B) in the roots of *col-0* seedlings treated with MHPP (40 μM or 80 μM) for up to 24 h. The fluorescence intensity of untreated roots was set to 100. For representative images, see Supplemental Fig. S6. (C) NO contents in the roots of *col-0* and *noa1* seedlings treated with or without MHPP (40 μM or 80 μM) for 24 h, as revealed by the NO-specific fluorescent probe DAF-2 DA. Bars, 50 μm. (D) Quantification of the NO-specific fluorescence intensity in plants treated as in (C). (E) ROS contents in the roots of *col-0* and *noa1* seedlings treated with or without MHPP (40 μM or 80 μM) for 24 h, as revealed by the ROS-specific fluorescent probe DCFH-DA. Bars, 50 μm. (F) Quantification of the ROS-specific fluorescence intensity in plants treated as in (E). The error bars represent the SEM. Different letters indicate significantly different values ($P < 0.05$ by Tukey's test).

seedlings exposed to MHPP alone at 2 d of treatment. We next analyzed PR growth in the *noa1* mutant upon MHPP treatment. Consistent with the results obtained from the pharmacological assay, *noa1* exhibited a less extensive reduction in PR elongation in the presence of 80 μM MHPP (Fig. 6G and 6H). These results suggest that NO is involved in the MHPP-mediated inhibition of PR growth.

We subsequently explored the possible involvement of ROS in the signal transduction of MHPP-induced morphological responses. We examined PR elongation in 5-d-old seedlings treated with 40 or 80 μM MHPP in the presence or absence of H_2O_2 or ROS scavengers KI or CAT for 2 d. The MHPP-mediated repression of PR growth was more extensive in seedlings supplemented with H_2O_2 (Fig. 7A and 7B) but was less extensive in seedlings supplemented with KI (Fig. 7C and 7D) or CAT (Fig. 7E and 7F). To verify the role of ROS in MHPP-mediated PR growth inhibition, ROS-deficient mutant lines were also examined. We found that the respiratory burst oxidase homolog mutants *rbohC* and *rbohD* and the double mutant *rbohD/F* exhibited a less extensive reduction in PR elongation than the wild-type *col-0* control in the presence of 80 μM MHPP (Fig. 8). These data indicate that MHPP treatment inhibits PR growth via NO-mediated ROS accumulation in root tips.

Based on the above results showing that MHPP inhibits PR growth by modulating meristematic cell division potential, we hypothesized that NO and ROS were involved

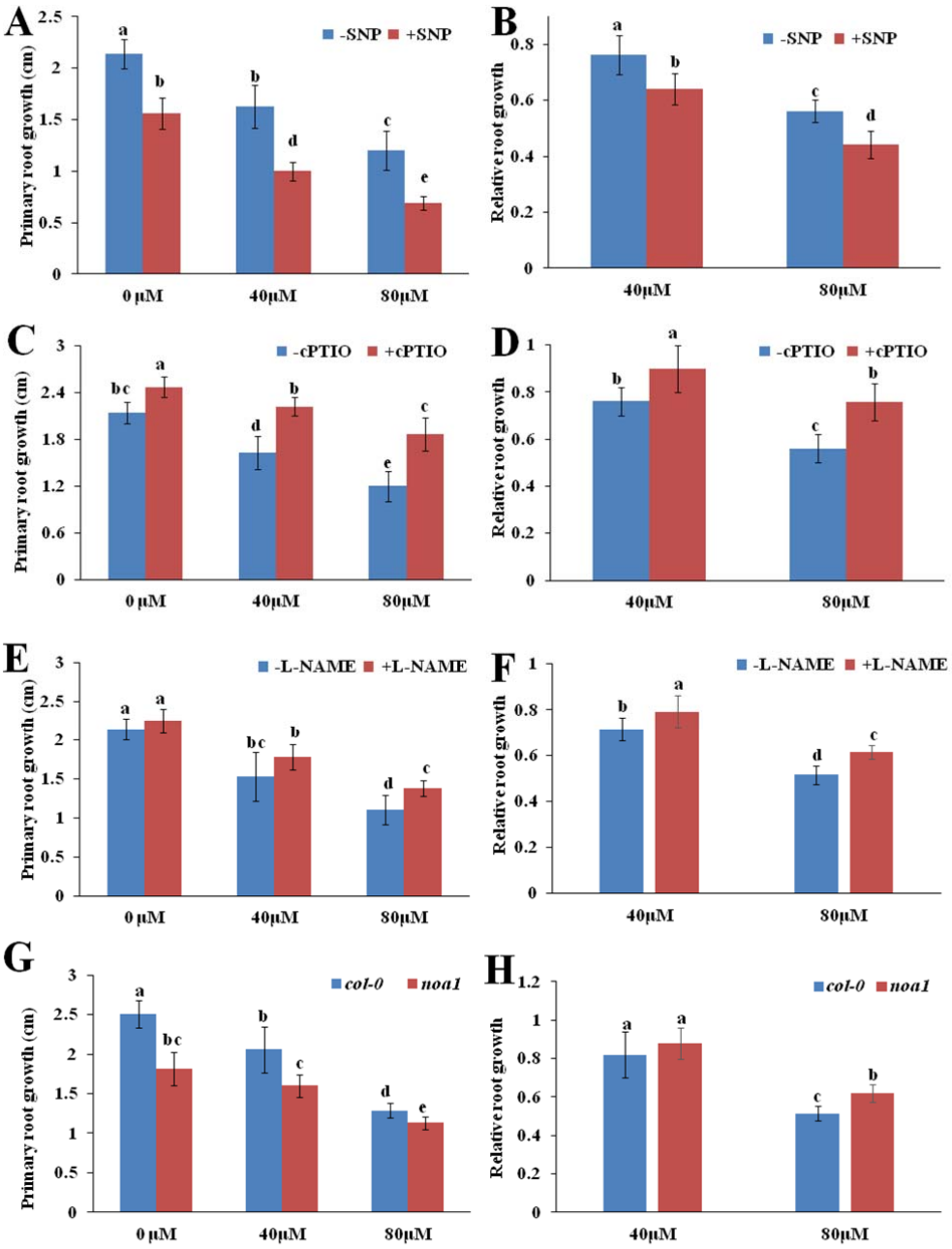

Fig. 6 (A-F) Primary root growth of *col-0* seedlings treated with or without MHPP (40 µM or 80 µM) for 2 d in the presence or absence of 100 µM SNP (A), 200 µM cPTIO (C) or 500 µM L-NAME (E). The data are presented relative to the control values obtained from *col-0* seedlings in the presence or absence of 100 µM SNP (B), 200 µM cPTIO (D) or 500 µM L-NAME (F). (G, H) Primary root growth of *col-0* and *noa1* seedlings treated with or without MHPP (40 µM or 80 µM) for 2 d (G) and the relative root growth of seedlings of the two genotypes treated with 40 µM or 80 µM MHPP compared with untreated seedlings (H). The error bars represent the SEM. Different letters indicate significantly different values ($P < 0.05$ by Tukey's test).

in MHPP-induced inhibition of meristematic cell division potential. Thus, we examined the effects of NO/ROS on meristematic cell division potential using the *CYCB1;1:GUS* marker line. GUS staining showed that supplementation with the NO scavenger cPTIO, the NO synthase (NOS) inhibitor L-NAME, or either ROS

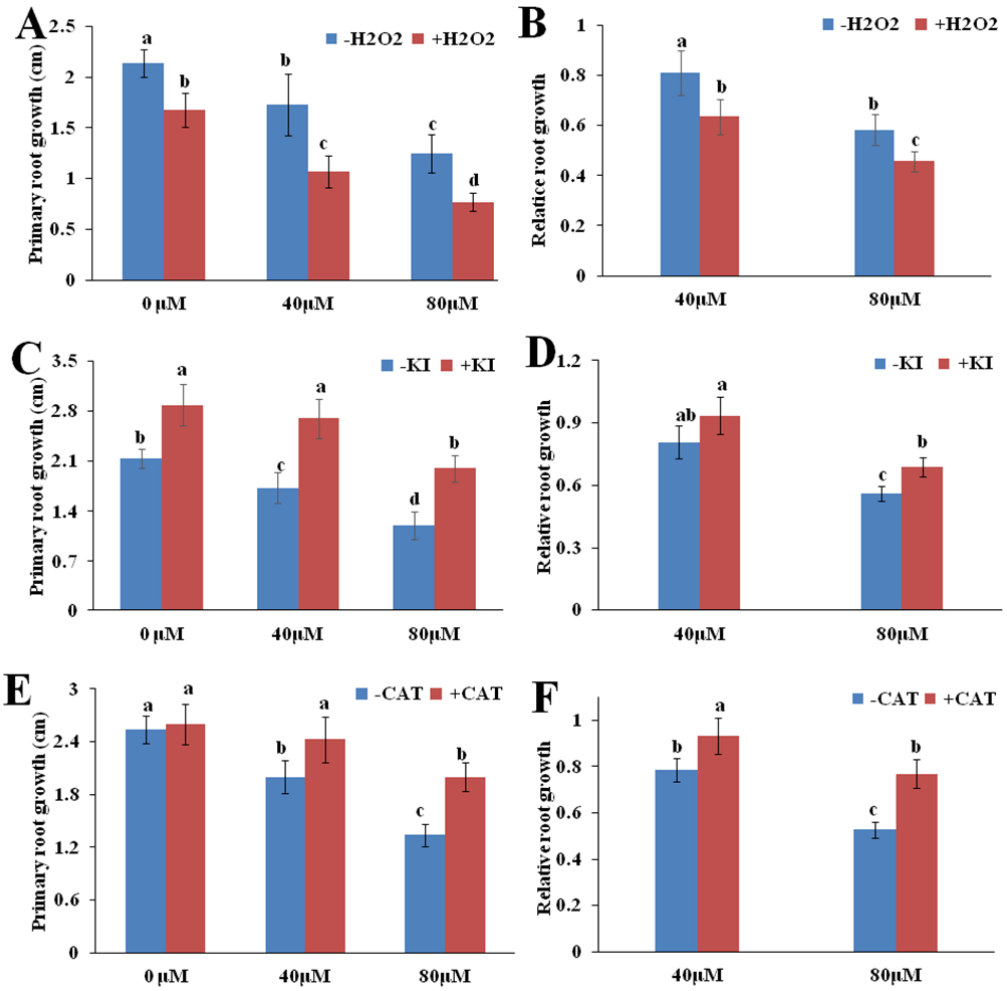

Fig. 7 (A-F) Primary root growth of *col-0* seedlings treated with or without MHPP (40 μM or 80 μM) for 2 d in the presence or absence of 500 μM H_2O_2 (A), 1 mM KI (C), or 200 μM CAT (E). The data are presented relative to the control values obtained from *col-0* seedlings in the presence or absence of 500 μM H_2O_2 (B), 1 mM KI (D), or 200 μM CAT (F). The error bars represent the SEM. Different letters indicate significantly different values ($P < 0.05$ by Tukey's test).

scavenger KI or CAT alleviated the overaccumulation of CYCB1;1 in roots caused by MHPP treatment (Fig. 9). However, supplementation with the NO donor SNP or H_2O_2 did not further increase CYCB1;1 accumulation in roots, perhaps because the MHPP-induced accumulation of NO and ROS in roots increased CYCB1;1 accumulation such that exogenous SNP or H_2O_2 application could not further enhance CYCB1;1 accumulation. These data indicate that NO and ROS are responsible for the MHPP-mediated inhibition of root meristem development.

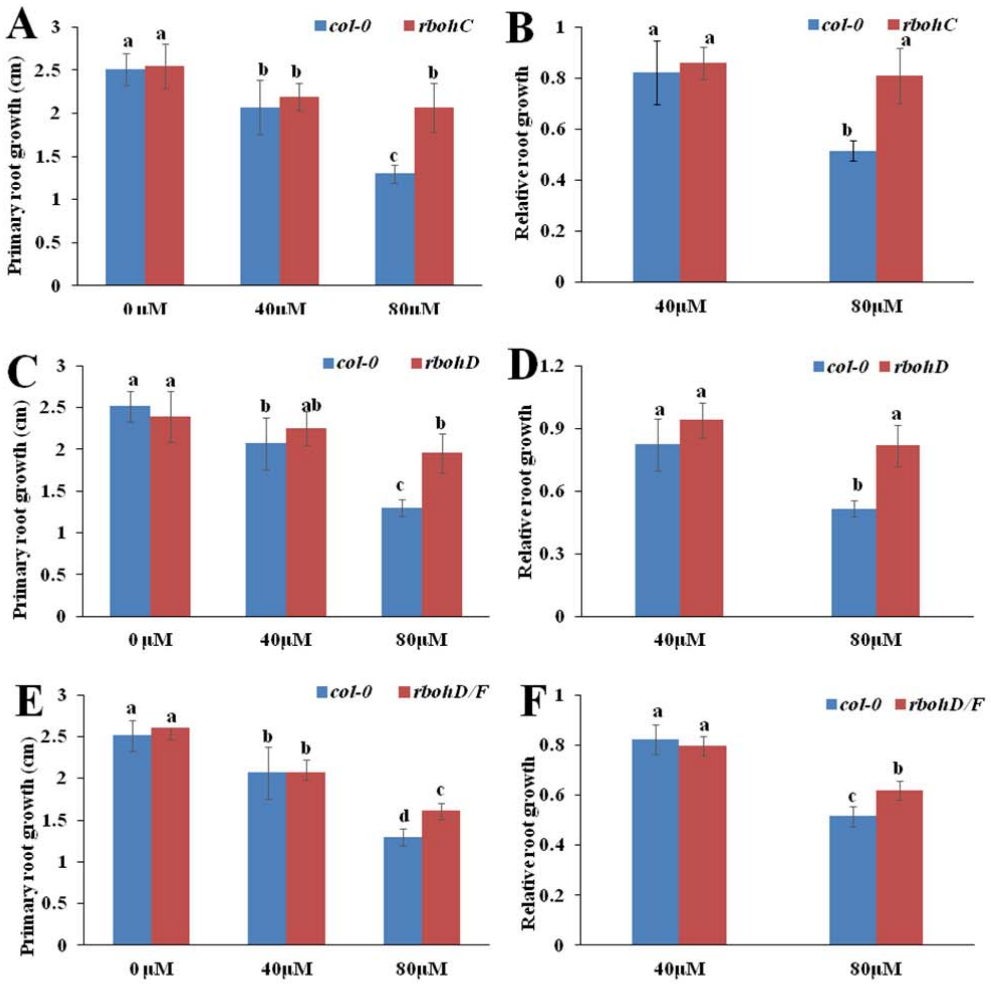

Fig. 8 (A, B) Primary root growth of *col-0* and *rbohC* seedlings treated with or without MHPP (40 μM or 80 μM) for 2 d (A) and the relative root growth of the two genotypes treated with 40 μM or 80 μM MHPP compared with untreated seedlings (B). (C, D) Primary root growth of *col-0* and *rbohD* seedlings treated with or without MHPP (40 μM or 80 μM) for 2 d (C) and the relative root growth of seedlings of the two genotypes treated with 40 μM or 80 μM MHPP compared with untreated seedlings (D). (E, F) Primary root growth of *col-0* and *rbohD/F* seedlings treated with or without MHPP (40 μM or 80 μM) for 2 d (E) and the relative root growth of seedlings of the two genotypes treated with 40 μM or 80 μM MHPP compared with untreated seedlings (F). The error bars represent the SEM. Different letters indicate significantly different values ($P < 0.05$ by Tukey's test).

NO-Mediated ROS Accumulation Was Possibly Responsible For MHPP-Induced Auxin Accumulation in Root Tips and Inhibition of Root Meristem Development

The above results show that MHPP inhibits PR elongation by increasing auxin accumulation in root tips. To determine whether MHPP-induced NO and ROS accumulation is involved in this process, we used the auxin-responsive *DR5:GFP* marker line to monitor the potential changes in auxin signaling in MHPP-treated seedlings in the presence or absence of an NO scavenger/inhibitor or an H_2O_2 scavenger. Exogenous addition of cPTIO or L-NAME reduced the expression of

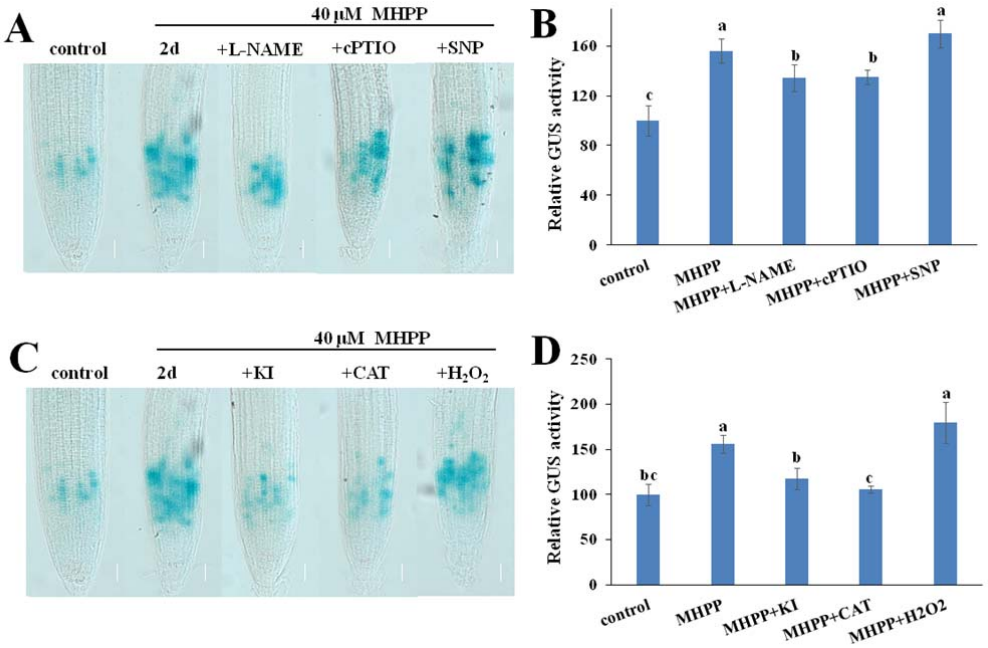

Fig. 9 NO and ROS are involved in the MHPP-mediated reduction of meristematic cell division potential. (A, B) Image of GUS staining of 5-d-old *CYCB1;1:GUS* seedlings exposed to 40 μM MHPP for 2 d in the presence or absence of 500 μM L-NAME, 200 μM cPTIO, or 100 μM SNP (A) and the relative GUS activity of *CYCB1;1:GUS* seedlings (B) treated as in (A). (C, D) Image of GUS staining of 5-d-old *CYCB1;1:GUS* seedlings exposed to 40 μM MHPP for 2 d in the presence or absence of 1 mM KI, 200 μM CAT, or 500 μM H_2O_2 (C) and the relative GUS activity of *CYCB1;1:GUS* seedlings (D) treated as in (C). Bars, 50 μm. The level of GUS activity in untreated roots was set to 100. The error bars represent the SEM. Different letters indicate significantly different values ($P < 0.05$ by Tukey's test).

DR5:GFP in MHPP-treated seedlings. Similarly, the H_2O_2 scavengers KI or CAT reduced, whereas exogenous H_2O_2 increased, the expression of this auxin reporter in MHPP-treated seedlings (Fig. 10A and 10B; for representative images, see Supplemental Figs. S9 and S10, respectively). To verify the role of NO/ROS in modulating the auxin levels, we used the auxin-perceptive marker line *DII-VENUS*. Exogenous application of an NO scavenger/inhibitor (cPTIO or L-NAME), or an H_2O_2 scavengers (KI or CAT) stabilized, whereas SNP or H_2O_2 further reduced, the fluorescence of the DII-VENUS marker in MHPP-treated seedlings (Fig. 10C and 10D; for representative images, see Supplemental Figs. S11 and S12, respectively). These data indicate that MHPP-induced NO acts as a second messenger to promote H_2O_2 production, thereby regulating root growth via the auxin pathway.

MHPP Induced the Accumulation of Glucosinolates in Arabidopsis Roots

To further investigate the role and molecular mechanisms of MHPP in modulating plant growth and development, we analyzed the transcript profiles in roots via high-throughput RNA-seq followed by qRT-PCR analysis. We compared the transcripts

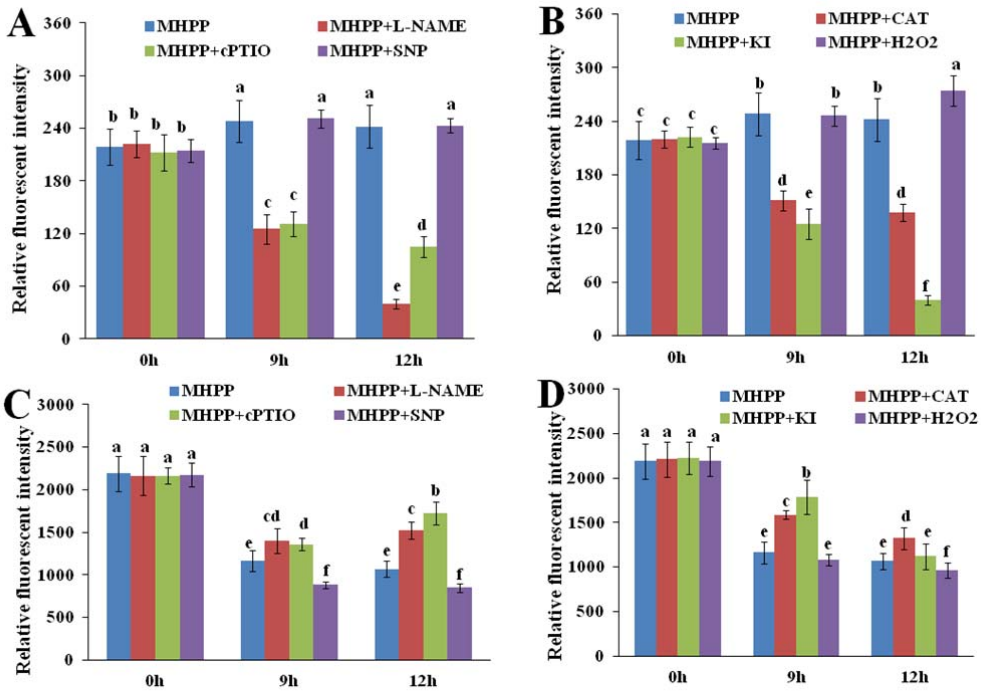

Fig. 10 NO and ROS are involved in the MHPP-mediated accumulation of auxin in root tips and inhibition of root meristem development. (A-D) Quantification of the DR5:GFP fluorescence intensity (A, B) and DII-VENUS fluorescence intensity (C, D) in the roots of *DR5:GFP* (A, B) or *DII-VENUS* (C, D) seedlings treated with or without 40 μM MHPP in the presence or absence of 500 μM L-NAME, 200 μM cPTIO, 100 μM SNP, 200 μM CAT, 1 mM KI, or 500 μM H_2O_2 for 9 or 12 h. For representative images, see Supplemental Fig. S9-S12.

obtained at 2 d in the presence of 40 or 80 μM MHPP. Relative to the gene expression levels under control conditions, 101 genes were down-regulated and 103 genes were up-regulated (altered by more than twofold) in roots treated with 40 μM MHPP, and 184 genes were down-regulated and 180 genes were up-regulated in roots treated with 80 μM MHPP (Log_2>1, FDR<0.01) (Supplemental Fig. S13). The differentially expressed genes showed enrichment in the KEGG pathway of glucosinolate biosynthesis due to either 40 or 80 μM MHPP treatment (Supplemental Fig. S14 and S15 and Table S1). We used qRT-PCR analysis to confirm the results of RNA-seq for the glucosinolate biosynthesis-related genes. The qRT-PCR analysis results strongly coincided with the RNA-seq results (R^2=0.6082); this finding verified the accuracy of the RNA-seq results (Supplemental Fig. S16A and S16B).

Because the above results showed that MHPP significantly induces the expression of glucosinolate biosynthesis-related genes, we evaluated the glucosinolate levels in MHPP-treated plants to determine whether the content of the glucosinolates was altered by MHPP treatment. As shown in Supplemental Fig. S16C, treated with MHPP significantly induces the accumulation of glucosinolates in roots.

Glucosinolates are a group of amino acid-derived metabolites (Shroff et al., 2008). Thus, we examined the contents of free amino acids in MHPP-treated plants. As shown in Supplemental Fig. S17, analysis of free amino acid contents revealed a large response to MHPP in *Arabidopsis* roots. MHPP treatment induced increases in the free amino acid levels in *Arabidopsis* roots. Among the seventeen amino acids evaluated, thirteen amino acids, including the precursors of glucosinolate biosynthesis L-phenylalanine (Phe), L-leucine (Leu), L-isoleucine (Ile), and L-tyrosine (Tyr), displayed higher levels, whereas only two amino acids (threonine (Thr) and histidine (His)) displayed lower levels, in the roots of seedlings treated with MHPP compared with untreated control seedlings. Two amino acids (valine (Val) and lysine (Lys)) showed similar concentrations in roots between plants treated with and without MHPP.

Glucosinolates are a class of typical chemical defense molecules in plants, and the glucosinolate biosynthesis pathway is induced by phytohormones such as jasmonic acid (JA) and salicylic acid (SA) (Van Dam et al., 2004; Tong et al., 2015). Therefore, we next assessed the levels of abscisic acid (ABA), JA, and SA in plants in response to MHPP treatment. As shown in Supplemental Fig. S18, treatment with MHPP significantly increased the contents of SA and JA by 212% and 627%, respectively, but did not affect the ABA level in the roots of MHPP-treated plants compared to control plants. These data imply that MHPP performs diverse functions in modulating plant growth, development and defense responses. The detailed molecular mechanisms underlying these functions require further investigation.

438

Discussion

MHPP Affects Root System Development by Modulating the Levels of Auxin Expression and Signaling

Early reports revealed that the phenolic substance MHPP, an exudate among the specific secondary organic compounds released from roots, possesses strong BNI activity (Subbarao et al. 2013). However, these previous studies focused on the inhibitory effects of MHPP on soil nitrification and nitrogen loss (Nardi et al., 2013), and the effects of MHPP on the root system growth and development have not been investigated. Several findings suggest that roots might also be targets of MHPP-mediated plant growth and development: (a) root-secreted secondary metabolites can regulate the growth and development of plants; (b) post-embryonic root development is an auxin-driven plastic process that rapidly adapts to external changes; and (c) MHPP treatment enhances nutrient uptake by plants. Here, we show that MHPP inhibits PR growth and promotes LR formation, thus modulating RSA remodeling. We first observed that MHPP inhibits PR elongation and LR formation in a dose-dependent manner. Because inhibition of root growth is a typical auxin signal phenotype, we hypothesized that MHPP impacts auxin signaling in roots, and we indeed found that MHPP treatment rapidly increased auxin accumulation in root tips.

Our results indicate that MHPP increases the expression of the DR5:GFP reporter in root tips by enhancing auxin biosynthesis, changing PAT and modulating auxin perception via the destabilization of the Aux/IAA family of transcriptional repressors in root tips. Several lines of evidence support these conclusions. First, GC/MS analysis confirmed elevated IAA contents in MHPP-treated plants, and at the molecular level, auxin biosynthesis-related genes were markedly up-regulated after MHPP treatment. Second, MHPP markedly affected the expression levels of PIN4, and genetic analysis supported the hypothesis that MHPP mediates auxin accumulation in root tips by affecting PAT via the modulation of PIN4. Third, the MHPP-mediated rapid degradation of Aux/IAA proteins was confirmed by examining DII-VENUS marker fluorescence and GUS staining of *HS:AXR3-GUS* plants. Fourth, physiologically, exogenous application of IAA enhanced the inhibitory effects of MHPP on PR growth, and genetic analysis supported this result in the auxin over-producing mutant *yucca* and the auxin-insensitive mutant *axr3-3*.

Proper auxin accumulation relies on the coordination between its biosynthesis and

transport (Liu et al., 2015). Treatment with the auxin transport inhibitor NPA or mutation of the *PIN* family of auxin carrier genes affects root growth (Blilou et al., 2005; Liu et al., 2015), and these observations suggest that disturbing PAT changes auxin accumulation in root tips and subsequently alters root growth. In this study, we found that NPA did not affect the MHPP-mediated inhibitory effects on PR elongation; this finding suggests that PAT is involved in MHPP-mediated root growth inhibition. Investigation of the expression levels of auxin carriers showed that MHPP significantly modulated the expression of PIN4. Furthermore, the *pin4-3* mutant exhibited reduced sensitivity to MHPP treatment in terms of PR growth, suggesting that PIN4 at least partly mediates MHPP-induced auxin accumulation to inhibit PR growth. PIN4 regulates auxin levels and gradients in the root meristem, and *pin4* mutant seedlings accumulate higher auxin levels in root tips (Friml et al., 2002). Our results indicated that MHPP treatment markedly reduced PIN4 expression and thereby disrupted auxin transport, thus leading to auxin accumulation in root tips. However, how PIN4 is involved in the MHPP-mediated modulation of PR growth remains to be explored.

Changes in Aux/IAA stability and, subsequently, the auxin perception level appear to represent a general strategy by which plants interplay with phytohormones and respond to environmental cues (Yuan et al., 2013; Bailly et al., 2014; Li et al., 2015; Liu et al., 2015; Yuan et al., 2016; Katz et al., 2015). Treatment with SA reduces auxin responses by stabilizing Aux/IAA proteins (Wang et al., 2007). Gain-of-function mutations of Aux/IAA proteins such as *IAA3* and *IAA17* induce defective root development (Hamann et al., 2002; Liu et al., 2015). We found that MHPP treatment enhanced the degradation of Aux/IAA proteins, as revealed by GUS staining of the *HS:AXR3-GUS* reporter line, and thereby amplified auxin signaling in root tips. We also observed reduced sensitivity of the *axr3-3* mutant to MHPP treatment compared with the WT control in terms of PR growth. MHPP treatment might not induce the degradation of mutant AXR3 in *axr3-3*, preventing MHPP from altering auxin signaling and subsequently inhibiting PR growth. Taken together, the results presented here clearly demonstrate that MHPP influences root growth by modulating the levels of auxin expression and signaling.

MHPP Affects Meristematic Cell Division Potential in Root Tips

505 Root growth is maintained by coordinating cell proliferation and differentiation. Root
506 tissue cells are derived from the stem cell niche, which is composed of an inner group
507 of mitotically inactive QC cells and an outer group of mitotically active stem cells
508 (Dinneny and Benfey, 2008; Ji et al., 2015). Root stem cell niche activity and
509 meristematic cell division potential are two crucial determinants of root meristem size
510 and root growth (Aida et al., 2004; Della Rovere et al., 2013; Ji et al., 2015). In this
511 study, we found that MHPP treatment did not change the expression levels of the QC
512 marker QC25:GUS. Both the *SHR*/*SCARECROW* (*SCR*) pathway and the *PLT*
513 pathway regulate QC identity and stem cell niche activity. *SHR* is primarily expressed
514 in the stele, and the encoded protein can move to the QC and other surrounding cells
515 to activate the expression of *SCR* together with *WOX5* to coordinately regulate QC
516 identity and the balance between root stem cell division and differentiation. The *PLT*
517 pathway modulates the auxin-dependent maintenance of the stem cell niche (Aida et
518 al., 2004; Galinha et al. 2007). Neither SHR nor PLT1 protein was altered in MHPP-
519 treated plants, and our finding suggests that MHPP treatment does not affect QC cell-
520 specific expression or RAM activity. Thus, we examined whether MHPP affects
521 meristematic cell division potential. Our results from GUS staining of the
522 *CYCB1;1:GUS* reporter line revealed that the percentage of GUS-stained cells in the
523 root meristem was significantly greater in MHPP-treated roots than in control roots.
524 These results imply that treatment with MHPP decelerated the cell cycle. These data
525 indicate that MHPP treatment inhibits PR growth by affecting meristematic cell
526 division potential but not stem cell niche activity.

527

528 **NO-Mediated ROS Accumulation in Root Tips Modifies the RSA in Response to**
529 **MHPP Treatment via the Auxin Pathway**

530 In this study, we obtained evidence for the involvement of ROS in NO signaling
531 during the response of plants to MHPP treatment. We found that treatment with
532 MHPP induced the accumulation of NO and ROS in roots. Supplementation with the
533 NO scavenger cPTIO or the NOS inhibitor L-NAME markedly inhibited ROS
534 accumulation, and this effect was also observed in the *noa1* mutant. In contrast,
535 supplementation with the ROS scavenger KI did not affect NO production in MHPP-
536 treated roots. These results suggest that NO acts upstream of ROS in the response of

plant roots to MHPP treatment. Pharmacological analysis using NO/ROS scavengers and genetic analysis using NO-/ROS-related mutants indicated that NO/ROS accumulation contributes to MHPP-mediated PR growth inhibition. Further investigation using the *CYCB1;1:GUS* reporter indicated that NO and ROS mediate the MHPP-induced inhibition of PR growth by reducing meristematic cell division potential.

Previous studies revealed that disrupting NO production reduced DR5:GUS expression in roots (Sanz et al., 2014). NO also affected auxin signaling by promoting the degradation of IAA17 (Terrile et al., 2012). In agreement with these findings, our study indicated that inhibition of NO production reduced the expression of the auxin-responsive reporter *DR5:GFP* but stabilized DII-VENUS marker fluorescence in MHPP-treated roots. Interestingly, Liu et al. (2015) found that NO reduced auxin responses and increased the stability of IAA17 in roots subjected to salt stress. The difference in these effects between studies may be due to the distinct stresses and environmental cues examined, as auxin responses and NO functions differ according to the type of stress or tissue.

ROS is another important signaling molecule that plays an important role in plant growth and environmental responses (Tsukagoshi et al., 2010). ROS regulates the balance between cellular proliferation and differentiation in roots (Tsukagoshi et al., 2010). It has been reported that the ROS and auxin pathways can extensively impact each other (Kwak et al. 2006). Interestingly, Blomster et al. (2011) found that O_3, an apoplastic form of ROS, transiently suppresses auxin signaling by reducing the gene expression of auxin receptors and the Aux/IAA family of transcriptional repressors. In this study, inhibiting H_2O_2 production reduced the expression of the auxin-responsive *DR5:GFP* reporter but stabilized DII-VENUS marker fluorescence in MHPP-treated roots, and our findings suggest that ROS contributes to the MHPP-mediated alterations in the levels of auxin expression and signaling in roots. The differences in these effects of ROS on auxin signaling between studies may be due to the distinct forms of ROS examined, as the response of plants to ROS varies depending on the form of ROS. Furthermore, these studies of the function of ROS in the plant response to environmental cues were based on the use of exogenous ROS donors. However, environmental cues, such as stresses, might induce endogenous ROS production; therefore, ROS might play specific roles in response to certain cues. In conclusion, our results indicate that MHPP treatment inhibits PR growth by increasing the NO

and ROS levels. The elevated accumulation of NO and ROS further altered the levels of auxin expression and perception to amplify auxin signaling.

The MHPP-Induced Accumulation of Plant Defense Molecules Implies its Diverse Functions in Modulating Plant Growth, Development, and Stress Tolerance

Glucosinolates, a group of sulfur-rich, amino acid-derived metabolites, are among the most extensively studied classes of antiherbivore defense chemicals in plants. Upon insect feeding or mechanical damage, glucosinolates are hydrolyzed into aglycone by myrosinase and subsequently form isothiocyanates, nitriles, and other products (Bones and Rossiter, 2006). These natural chemicals, which most likely contribute to plant defense against pests and diseases, are also detected in small amounts in humans and are believed to contribute to the health-promoting properties of cruciferous vegetables (Halkier and Gershenzon, 2006; Shroff et al., 2008). Interestingly, MHPP treatment induced the accumulation of glucosinolates and their amino acid precursors in roots. We also observed significantly elevated levels of two defense signaling phytohormones, SA and JA, in MHPP-treated plants. These data suggest that MHPP induces the production of plant defense-related metabolites and that MHPP might promote antiherbivore defense responses in plants. Further studies will focus on how MHPP elevates the levels of JA and SA and whether the MHPP-induced accumulation of JA and SA is involved in the enhancement of glucosinolate production in plants.

In this study, we also found that MHPP treatment promoted LR development. LR formation is tightly mediated by the auxin pathway (Li et al., 2015). The induction of the expression of IAA biosynthesis-related genes in seedlings and the increase in the IAA content in roots might be partly explain the enhancement of LR development in response to MHPP treatment. However, the detailed molecular mechanisms involved in MHPP-induced LR formation and whether the changes in the expression of PIN4 are also involved in MHPP-induced LR development remain to be further explored. Increased LR formation altered RSA, ultimately benefiting the uptake of water and nutrient elements into roots. Indeed, we found that MHPP markedly increased the contents of nutrient elements in seedlings, including P, K, S, Fe, Mn, Zn, and Cu. This observation indicated that MHPP enhanced nutrient element accumulation in plants. Further studies will examine whether MHPP could regulate the expression of the

transporters of nutrient elements and metal ions in plants and affect the transport of nutrient elements from the roots to above-ground portions of plants.

In conclusion, our data indicate that MHPP, in addition its function as a nitrification inhibitor, profoundly impacts root development. Based on our results, MHPP inhibits PR elongation by regulating the levels of auxin expression, transport, and signaling in roots and consequently altering root meristematic cell division potential, and the NO/ROS pathway is involved in these processes. Moreover, treatment with MHPP increases nutrient element uptake and plant defense-related metabolite accumulation in roots. Although the possible involvement of other pathways in MHPP-induced RSA remodeling remains to be explored, our findings show that MHPP modulates plant growth, development, and stress tolerance by inducing morphological and physiological changes in roots. Further research examining the interplay of MHPP with phytohormones will enable a broader understanding of the mechanism by which plants respond to MHPP by regulating hormonal signaling, will aid in the development of cost-effective, sustainable agricultural strategies for crop breeding and cultivation, and will provide insight into novel applications of this biological nitrification inhibitor.

Materials and Methods

Plant Growth and Chemical Treatments

Arabidopsis seedlings of the following lines were used in this study: *Columbia-0* (*col-0*), the mutants *yucca*, *pin4-3*, *axr3-3*, *axr1-12*, *noa1*, *rbohC*, *rbohD*, *rbohD/F*, *pin1*, *pin2*, *pin7-2*, and *aux1-21* on a *col-0* background, and the transgenic lines *DR5:GFP*, *PIN1:PIN1-GFP*, *PIN2:PIN2-GFP*, *PIN4:PIN4-GFP*, *PIN7:PIN7-GFP*, *AUX1:AUX1-YFP*, *PLT1:PLT1-GFP*, *SHR:SHR-GFP*, *DII-VENUS*, *mDII-VENUS,* *QC25:GUS*, *CYCB1;1:GUS*, *HS:AXR3NT-GUS*, and *HS:GUS*.

Seeds were surface-sterilized and plated on agar medium containing 1/2 MS medium (Sigma), pH 5.75, supplemented with 1% agar and 10% sucrose. Seedlings were grown in a vertical position in a growth chamber maintained at 22°C under a 16/8 h light/dark cycle. Five-day-old seedlings were transferred to plates supplemented with various chemicals, such as MHPP, IAA, NPA, SNP, c-PTIO, and L-NAME, and grown for an additional 2-5 d. All chemicals were obtained from Sigma-Aldrich.

GUS Staining

To detect the expression of GUS, we incubated *QC25:GUS* or *CYCB1;1:GUS* seedlings in GUS buffer containing the substrate 1 mM X-Gluc (5-bromo-4-chloro-3-indolyl-β-D-glucuronic acid cyclohexyl-ammonium, Sigma) at 37°C in the dark (Ulmasov et al. 1997). The GUS staining duration was dependent on the transgenic marker line: 5 h for *QC25:GUS* and 3 h for *CYCB1;1:GUS*. MUG assays were performed according to a previously described method (Cote et al., 2003). The seedlings were washed and placed in 75% (w/v) ethanol before examination under a microscope (Zeiss Axioskop). At least 20 seedlings were analyzed for each treatment. The experiments were repeated at least three times.

Measurement of the Production of NO and H_2O_2

The endogenous NO levels in root meristems were visualized using the NO-specific fluorescent probe DAF-2 DA (Beyotime, China). Seedlings were incubated at 37°C in 5 μM staining solution for 1 h. Then, the samples were washed twice and viewed under a Leica laser scanning confocal microscope (excitation, 490 nm; emission, 515 nm). Quantitative measurement of fluorescence intensity was performed using ImageJ. The endogenous H_2O_2 levels in root meristems were visualized using the H_2O_2-specific fluorescent probe DCFH-DA (Beyotime). Seedlings were incubated at 37°C in 10 μM staining solution for 5 min. Then, the samples were washed twice and viewed under a Leica laser scanning confocal microscope (excitation, 488 nm; emission, 530 nm). Quantitative measurement of fluorescence intensity was performed using ImageJ.

Phenotypic Analysis

Relative root growth was calculated as the length of root growth under the treatment conditions divided by the mean root length under control conditions as described by Freeman *et al.* (2010). At least 15 replicate plants were measured for each treatment. Measurements of the lengths of meristem zones and elongation zones and the average cell length in the differentiation zone were outperformed according to published methods (Dello Ioio et al., 2007; Yuan et al., 2013; Liu et al., 2015). LRP initiation was quantified in roots using the *DR5:GUS* reporter line. The four developmental stages of the LRP were classified as follows: up to three cell layers (stage A); more than three cell layers but non-emerged (stage B); emerged LRs <0.5 mm in length (stage

672 C); and emerged LRs >0.5 mm in length (stage D) (Zhang et al., 1999; Li et al., 2005).
673 Only mature LRs (>0.5 mm) are denoted as LRs.
674
675 **qRT-PCR Analysis**
676 Seedlings were collected for total RNA isolation using TRIzol Reagent (TaKaRa)
677 according to the manufacturer's instructions. The RNA concentration was accurately
678 quantified using spectrophotometry. Then, cDNA was synthesized from DNase-
679 treated total RNA (1 μg) using a Reverse Transcription System Kit (Promega) and
680 oligo(dT) primers. The cDNA produced was diluted 1:15, and 3 μL of diluted cDNA
681 was employed for qRT-PCR in a 7500 Real Time System (Applied Biosystems) using
682 Platinum® SYBR® Green qPCR SuperMix-UDG (Invitrogen). *ACTIN2*
683 (AT3G18780) and *EF1a* (AT5G60390) were used as internal controls for qRT-PCR
684 normalization using GeNorm (Czechowski et al., 2005). For each gene, qRT-PCR
685 was performed on three biological replicates, with duplicates for each biological
686 replicate. The relative transcript level was determined for each sample and was
687 averaged over the six replicates. The specific primers used for each gene are listed in
688 Supplemental Table S2. All primer pairs produced only one peak in DNA melting
689 curves, and this result indicated the high specificity of the primers.
690
691 **Quantification of IAA Content**
692 IAA content was quantified according to Gao et al. (2014) and Liu et al. (2015). Root
693 tips of approximately 0.1 g fresh weight were collected and immediately frozen in
694 liquid nitrogen. After extraction, endogenous IAAs were purified, methylated in a
695 stream of diazomethane gas and resuspended in 100 μL of ethyl acetate. The
696 endogenous IAA content was analyzed by GC/MS.
697
698 **Nutrient Element Contents Analysis**

699 Seedlings grown in 1/2 MS medium were treated with 40 μM MHPP for 2 d. The
700 treated roots were immersed in a solution containing 1 mM EDTA for 2 h and then
701 thoroughly rinsed with distilled water. The dried plant tissues were ground and
702 digested in concentrated nitric acid for 2 d at room temperature. Next, the samples
703 were boiled for 2 h until completely digested. After adding 3 mL of Millipore-filtered
704 deionized water and brief centrifugation, the contents of Zn, Fe, Mn and Cu were

705 determined using ICP-MS, and the contents of P, K, and S were determined using
706 ICP-AES. Each experiment was repeated three times.

707

708 **Statistical Analysis**

709 For each treatment, at least 12 roots were analyzed; all experiments were repeated at
710 least three times. The results are presented as the means ± SEM. For statistical
711 analysis, we used Tukey's test ($P<0.01$).

712

713 **Acknowledgements**
714 The authors would like to thank Prof. Shaojian Zheng (Zhejiang University) for
715 providing *yucca* seeds, Prof. Yingtang Lu (Wuhan University) and Dr. Hongmei Yuan
716 (Hainan University) for providing *pin1* seeds, and the Arabidopsis Biological
717 Resource Center for the mutant seeds. We truly appreciate Prof. Zhaojun Ding
718 (Shandong University) for his helpful discussion and guidance. The authors gratefully
719 acknowledge the Central Laboratory of the Xishuangbanna Tropical Botanical Garden
720 for providing research facilities.

721

722 **Supplemental Data**
723 The following materials are available in the online version of this article
724 **Tab. S1** Differential expression gene involved in glucosinolate biosynthesis

725 **Table S2.** List of the primers for qRT-PCR analysis of the genes

726 **Fig. S1** Effects of MHPP on root meristem development.

727 **Fig. S2** GFP fluorescence in the roots of *DR5:GFP* or *PIN4:GFP* seedlings.

728 **Fig. S3** GFP/YFP fluorescence in the roots of *PIN1/2/7:GFP* and
729 *AUX1:YFP*seedlings.

730 **Fig. S4** Relative root growth of seedlings exposed to MHPP.

731 **Fig. S5** YFP fluorescence in the roots of *DII-VENUS* or *mDII-VENUS* seedlings.

Fig. S6 Detection of NO and H_2O_2 production.

Fig. S7 ROS and NO in the roots of wild-type seedlings response to MHPP.

Fig. S8 Image of DAB staining.

Fig. S9 GFP fluorescence in the roots of *DR5:GFP* seedlings (1).

Fig. S10 GFP fluorescence in the roots of *DR5:GFP* seedlings (2).

Fig. S11 YFP fluorescence in the roots of *DII-VENUS* seedlings (1).

Fig. S12 YFP fluorescence in the roots of *DII-VENUS* seedlings (2).

Fig. S13 Hierarchical clustering analysis.

Fig. S14 KEGG pathway enrichment analysis.

Fig. S15 Modulation of glucosinolate biosynthesis after MHPP treatment.

Fig. S16 MHPP up-regulates several genes involved in glucosinolate biosynthesis.

Fig. S17 MHPP affects the free amino acid contents.

Fig. S18 The contents of ABA, SA, and JA.

Figure Legends

Fig.1 MHPP affected root system development in *Arabidopsis*. (A-G) Five-day-old wild-type seedlings grown in 1/2 MS medium were treated with 40 or 80 μM MHPP for 5 d (A). Bar, 0.5 cm. Primary root elongation (B), the lengths of meristem zones (C) and elongation zones (D), the average cell length in the differentiation zone (E), the number of lateral roots (F), and lateral root primordium initiation (G) were measured after 5 d of treatment. (H,I) Image of GUS staining in 5-d-old *CYCB1;1:GUS* seedlings exposed to 40 μM MHPP for 3-48 h (H) and the relative GUS activity of *CYCB1;1:GUS* seedlings (I) treated as in (H). Bars, 50 μm. The level of GUS activity in untreated roots was set to 100. The error bars represent the SEM. Different letters indicate significantly different values ($P < 0.05$ by Tukey's test). (J) Nutrient element contents in MHPP-treated *Arabidopsis* seedlings. The ± symbol represents the SEM. The asterisks indicate significant differences with respect to the corresponding control based on Tukey's test (*, $0.01<P<0.05$; **, $P<0.01$).

Fig. 2 MHPP treatment enhanced auxin accumulation in roots, thus inhibiting primary root growth. (A) IAA contents in the roots of *col-0* seedlings and *yucca* seedlings treated with or without 40 μM MHPP for 24 h. (B,C) GFP fluorescence in the roots of 5-d-old *DR5:GFP* seedlings exposed to 40 μM MHPP for 9-24 h (B) and quantification of *DR5:GFP* fluorescence intensity (C) in plants treated as in (B). The fluorescence intensity of untreated roots was set to 100. Bars, 50 μm. (D) Quantitative real-time reverse transcription-polymerase chain reaction (qRT-PCR) analysis of the gene expression of auxin biosynthesis-related genes in *col-0* seedlings treated with or without 40 μM MHPP for 12 h. The expression levels of the indicated genes in untreated roots were set to 1. (E) Primary root growth of *col-0* seedlings treated with or without MHPP (40 μM or 80 μM) in the presence of 0 or 0.5 nM IAA for 2 d. (F, G) Primary root growth of *col-0* seedlings and *yucca* seedlings treated with or without MHPP (40 μM or 80 μM) for 2 d (F) and the relative root growth of seedlings of the two genotypes treated with 40 μM or 80 μM MHPP compared with untreated seedlings (G). (H) Primary root growth of wild-type seedlings treated with or without 40 μM MHPP in the presence or absence of 1 μM NPA for 2 d. The error bars represent the SEM. The asterisks (**) indicate significant differences with respect to

778 the corresponding control (P<0.01 based on Tukey's test). Different letters indicate
779 significantly different values (P < 0.05 by Tukey's test).

780

781 **Fig. 3** PIN4 plays a role in the MHPP-mediated inhibition of primary root growth. (A)
782 Quantitative real-time reverse transcription-polymerase chain reaction (qRT-PCR)
783 analysis of the gene expression of auxin carrier genes in the roots of *col-0* seedlings
784 treated with or without 40 μM MHPP for 12 h. The expression levels of the indicated
785 genes in untreated roots were set to 1. (B,C) GFP fluorescence in the roots of 5-d-old
786 *PIN4:GFP* seedlings exposed to 40 μM MHPP for 3-48 h (B) and quantification of
787 the *PIN4:GFP* fluorescence intensity (C) in plants treated as in (B). Bars, 50 μm. (D,
788 E) Primary root growth of *col-0* and *pin4-3* seedlings treated with or without MHPP
789 (40 μM or 80 μM) for 2 d (D) and the relative root growth of seedlings of the two
790 genotypes treated with 40 μM or 80 μM MHPP compared with untreated seedlings
791 (E). The error bars represent the SEM. The asterisks (**) indicate significant
792 differences with respect to the corresponding control (P<0.01 based on Tukey's test).
793 Different letters indicate significantly different values (P < 0.05 by Tukey's test).

794

795 **Fig. 4** MHPP treatment reduces the stability of Aux/IAA proteins. (A) Relative root
796 growth of wild-type seedlings treated with MHPP (40 μM or 80 μM) in the presence
797 or absence of 100 μM PCIB for 2 d. The length of untreated roots of *col-0* plants was
798 set to 1. (B,D) YFP fluorescence in the roots of 5-d-old *DII-VENUS* seedlings
799 exposed to 40 μM MHPP for 9 or 24 h (B) and quantification of the *DII-VENUS*
800 fluorescence intensity (D) in plants treated as in (B). Bars, 50 μm. The fluorescence
801 intensity of untreated roots was set to 100. (C) Image of GUS staining of 5-d-old
802 *HS:AXR3NT-GUS* seedlings. The seedlings were heat-shocked at 37°C for 2 h and
803 then treated with or without 40 μM MHPP for 45 min at 23°C, followed by GUS
804 staining. Bars, 50 μm. (E) The relative GUS activity of *HS:AXR3NT-GUS* seedlings
805 treated as in (C). The level of GUS activity in untreated roots was set to 100. (F,G)
806 Primary root growth of *col-0* and *axr3-3* seedlings treated with or without MHPP (40
807 μM or 80 μM) for 2 d (F) and the relative root growth of seedlings of the two
808 genotypes treated with 40 μM or 80 μM MHPP compared with untreated seedlings

809 (G). The error bars represent the SEM. Different letters indicate significantly different
810 values ($P < 0.05$ by Tukey's test).

811

812 **Fig. 5** NO and ROS are involved in the MHPP-mediated inhibition of primary root
813 growth. (A,B) Quantification of the NO-specific fluorescence intensity (A) and ROS-
814 specific fluorescence intensity (B) in the roots of *col-0* seedlings treated with MHPP
815 (40 μM or 80 μM) for up to 24 h. The fluorescence intensity of untreated roots was set
816 to 100. For representative images, see Supplemental Fig. S6. (C) NO contents in the
817 roots of *col-0* and *noa1* seedlings treated with or without MHPP (40 μM or 80 μM)
818 for 24 h, as revealed by the NO-specific fluorescent probe DAF-2 DA. Bars, 50 μm.
819 (D) Quantification of the NO-specific fluorescence intensity in plants treated as in (C).
820 (E) ROS contents in the roots of *col-0* and *noa1* seedlings treated with or without
821 MHPP (40 μM or 80 μM) for 24 h, as revealed by the ROS-specific fluorescent probe
822 DCFH-DA. Bars, 50 μm. (F) Quantification of the ROS-specific fluorescence
823 intensity in plants treated as in (E). The error bars represent the SEM. Different letters
824 indicate significantly different values ($P < 0.05$ by Tukey's test).

825

826 **Fig. 6** (A-F) Primary root growth of *col-0* seedlings treated with or without MHPP
827 (40 μM or 80 μM) for 2 d in the presence or absence of 100 μM SNP (A), 200 μM
828 cPTIO (C) or 500 μM L-NAME (E). The data are presented relative to the control
829 values obtained from *col-0* seedlings in the presence or absence of 100 μM SNP (B),
830 200 μM cPTIO (D) or 500 μM L-NAME (F). (G, H) Primary root growth of *col-0* and
831 *noa1* seedlings treated with or without MHPP (40 μM or 80 μM) for 2 d (G) and the
832 relative root growth of seedlings of the two genotypes treated with 40 μM or 80 μM
833 MHPP compared with untreated seedlings (H). The error bars represent the SEM.
834 Different letters indicate significantly different values ($P < 0.05$ by Tukey's test).

835

836 **Fig. 7** (A-F) Primary root growth of *col-0* seedlings treated with or without MHPP
837 (40 μM or 80 μM) for 2 d in the presence or absence of 500 μM H_2O_2 (A), 1 mM KI
838 (C), or 200 μM CAT (E). The data are presented relative to the control values
839 obtained from *col-0* seedlings in the presence or absence of 500 μM H_2O_2 (B), 1 mM

KI (D), or 200 μM CAT (F). The error bars represent the SEM. Different letters indicate significantly different values ($P < 0.05$ by Tukey's test).

Fig. 8 (A, B) Primary root growth of *col-0* and *rbohC* seedlings treated with or without MHPP (40 μM or 80 μM) for 2 d (A) and the relative root growth of the two genotypes treated with 40 μM or 80 μM MHPP compared with untreated seedlings (B). (C, D) Primary root growth of *col-0* and *rbohD* seedlings treated with or without MHPP (40 μM or 80 μM) for 2 d (C) and the relative root growth of seedlings of the two genotypes treated with 40 μM or 80 μM MHPP compared with untreated seedlings (D). (E, F) Primary root growth of *col-0* and *rbohD/F* seedlings treated with or without MHPP (40 μM or 80 μM) for 2 d (E) and the relative root growth of seedlings of the two genotypes treated with 40 μM or 80 μM MHPP compared with untreated seedlings (F). The error bars represent the SEM. Different letters indicate significantly different values ($P < 0.05$ by Tukey's test).

Fig. 9 NO and ROS are involved in the MHPP-mediated reduction of meristematic cell division potential. (A, B) Image of GUS staining of 5-d-old *CYCB1;1:GUS* seedlings exposed to 40 μM MHPP for 2 d in the presence or absence of 500 μM L-NAME, 200 μM cPTIO, or 100 μM SNP (A) and the relative GUS activity of *CYCB1;1:GUS* seedlings (B) treated as in (A). (C, D) Image of GUS staining of 5-d-old *CYCB1;1:GUS* seedlings exposed to 40 μM MHPP for 2 d in the presence or absence of 1 mM KI, 200 μM CAT, or 500 μM H_2O_2 (C) and the relative GUS activity of *CYCB1;1:GUS* seedlings (D) treated as in (C). Bars, 50 μm. The level of GUS activity in untreated roots was set to 100. The error bars represent the SEM. Different letters indicate significantly different values ($P < 0.05$ by Tukey's test).

Fig. 10 NO and ROS are involved in the MHPP-mediated accumulation of auxin in root tips and inhibition of root meristem development. (A-D) Quantification of the DR5:GFP fluorescence intensity (A, B) and DII-VENUS fluorescence intensity (C, D) in the roots of *DR5:GFP* (A, B) or *DII-VENUS* (C, D) seedlings treated with or without 40 μM MHPP in the presence or absence of 500 μM L-NAME, 200 μM

871 cPTIO, 100 μM SNP, 200 μM CAT, 1 mM KI, or 500 μM H_2O_2 for 9 or 12 h. For
872 representative images, see Supplemental Fig. S9-S12.

873

874

875

876

Parsed Citations

Aida M, Beis D, Heidstra R, Willemsen V, Blilou I, Galinha C, Nussaume L, Noh YS, Amasino R, Scheres B (2004) The PLETHORA genes mediate patterning of the Arabidopsis root stem cell niche. Cell 119: 109-120

Pubmed: Author and Title
CrossRef: Author and Title
Google Scholar: Author Only Title Only Author and Title

Bailly A, Groenhagen U, Schulz S, Geisler M, Eberl L, Weisskopf L (2014) The inter-kingdom volatile signal indole promotes root development by interfering with auxin signalling. Plant J 80: 758-771

Pubmed: Author and Title
CrossRef: Author and Title
Google Scholar: Author Only Title Only Author and Title

Baluska F, Mancuso S, Volkmann D, Barlow PW (2010) Root apex transition zone: a signalling-response nexus in the root. Trends Plant Sci 15: 402-408

Pubmed: Author and Title
CrossRef: Author and Title
Google Scholar: Author Only Title Only Author and Title

Bashandy T, Guilleminot J, Vernoux T, Caparros-Ruiz D, Ljung K, Meyer Y, Reichheld JP (2010) Interplay between the NADP-Linked Thioredoxin and Glutathione Systems in Arabidopsis Auxin Signaling. Plant Cell 22: 376-391

Pubmed: Author and Title
CrossRef: Author and Title
Google Scholar: Author Only Title Only Author and Title

Blilou I, Xu J, Wildwater M, Willemsen V, Paponov I, Friml J, Heidstra R, Aida M, Palme K, Scheres B (2005) The PIN auxin efflux facilitator network controls growth and patterning in Arabidopsis roots. Nature 433: 39-44

Pubmed: Author and Title
CrossRef: Author and Title
Google Scholar: Author Only Title Only Author and Title

Blomster T, Salojarvi J, Sipari N, Brosche M, Ahlfors R, Keinanen M, Overmyer K, Kangasjarvi J (2011) Apoplastic Reactive Oxygen Species Transiently Decrease Auxin Signaling and Cause Stress-Induced Morphogenic Response in Arabidopsis. Plant Physiol 157: 1866-1883

Pubmed: Author and Title
CrossRef: Author and Title
Google Scholar: Author Only Title Only Author and Title

Bones AM, Rossiter JT (2006) The enzymic and chemically induced decomposition of glucosinolates. Phytochemistry 67: 1053-1067

Pubmed: Author and Title
CrossRef: Author and Title
Google Scholar: Author Only Title Only Author and Title

Brunoud G, Wells DM, Oliva M, Larrieu A, Mirabet V, Burrow AH, Beeckman T, Kepinski S, Traas J, Bennett MJ, Vernoux T (2012) A novel sensor to map auxin response and distribution at high spatio-temporal resolution. Nature 482: 103-106

Pubmed: Author and Title
CrossRef: Author and Title
Google Scholar: Author Only Title Only Author and Title

Colon-Carmona A, You R, Haimovitch-Gal T, Doerner P (1999) Spatio-temporal analysis of mitotic activity with a labile cyclin-GUS fusion protein. Plant J 20: 503-508

Pubmed: Author and Title
CrossRef: Author and Title
Google Scholar: Author Only Title Only Author and Title

Correa-Aragunde N, Graziano M, Lamattina L (2004) Nitric oxide plays a central role in determining lateral root development in tomato. Planta 218: 900-905

Pubmed: Author and Title
CrossRef: Author and Title
Google Scholar: Author Only Title Only Author and Title

Cote C, Rutledge RG (2003) An improved MUG fluorescent assay for the determination of GUS activity within transgenic tissue of woody plants. Plant Cell Rep 21: 619-624

Pubmed: Author and Title
CrossRef: Author and Title
Google Scholar: Author Only Title Only Author and Title

Czechowski T, Stitt M, Altmann T, Udvardi MK, Scheible WR (2005) Genome-wide identification and testing of superior reference genes for transcript normalization in Arabidopsis. Plant Physiol 139: 5-17

Pubmed: Author and Title
CrossRef: Author and Title
Google Scholar: Author Only Title Only Author and Title

Della Rovere F, Fattorini L, D'Angeli S, Veloccia A, Falasca G, Altamura MM (2013) Auxin and cytokinin control formation of the quiescent centre in the adventitious root apex of arabidopsis. Ann Bot 112: 1395-1407

Pubmed: Author and Title
CrossRef: Author and Title
Google Scholar: Author Only Title Only Author and Title

Dello Ioio R, Linhares FS, Scacchi E, Casamitjana-Martinez E, Heidstra R, Costantino P, Sabatini S (2007) Cytokinins determine Arabidopsis root-meristem size by controlling cell differentiation. Curr Biol 17: 678-682
Pubmed: Author and Title
CrossRef: Author and Title
Google Scholar: Author Only Title Only Author and Title

Dinneny JR, Benfey PN (2008) Plant stem cell niches: Standing the test of time. Cell 132: 553-557
Pubmed: Author and Title
CrossRef: Author and Title
Google Scholar: Author Only Title Only Author and Title

Fan SC, Lin CS, Hsu PK, Lin SH, Tsay YF (2009) The Arabidopsis Nitrate Transporter NRT1.7, Expressed in Phloem, Is Responsible for Source-to-Sink Remobilization of Nitrate. Plant Cell 21: 2750-2761
Pubmed: Author and Title
CrossRef: Author and Title
Google Scholar: Author Only Title Only Author and Title

Fernandez-Marcos M, Sanz L, Lewis DR, Muday GK, Lorenzo O (2011) Nitric oxide causes root apical meristem defects and growth inhibition while reducing PIN-FORMED 1 (PIN1)-dependent acropetal auxin transport. Proc Natl Acad Sci USA 108: 18506-18511
Pubmed: Author and Title
CrossRef: Author and Title
Google Scholar: Author Only Title Only Author and Title

Freeman JL, Tamaoki M, Stushnoff C, Quinn CF, Cappa JJ, Devonshire J, Fakra SC, Marcus MA, McGrath SP, Van Hoewyk D, Pilon-Smits EA (2010) Molecular mechanisms of selenium tolerance and hyperaccumulation in Stanleya pinnata. Plant Physiol 153: 1630-1652
Pubmed: Author and Title
CrossRef: Author and Title
Google Scholar: Author Only Title Only Author and Title

Friml J, Benková E, Blilou I, Wisniewska J, Hamann T, Ljung K, Woody S, Sandberg G, Scheres B, Jurgens G, Palme K (2002). AtPIN4 mediates sink-driven auxin gradients and root patterning in Arabidopsis. Cell 108: 661-673
Pubmed: Author and Title
CrossRef: Author and Title
Google Scholar: Author Only Title Only Author and Title

Galinha C, Hofhuis H, Luijten M, Willemsen V, Blilou I, Heidstra R, Scheres B (2007) PLETHORA proteins as dose-dependent master regulators of Arabidopsis root development. Nature 449: 1053-1057
Pubmed: Author and Title
CrossRef: Author and Title
Google Scholar: Author Only Title Only Author and Title

Gao X, Yuan HM, Hu YQ, Li J, Lu YT (2014) Mutation of Arabidopsis CATALASE2 results in hyponastic leaves by changes of auxin levels. Plant Cell Environ 37: 175-188
Pubmed: Author and Title
CrossRef: Author and Title
Google Scholar: Author Only Title Only Author and Title

Gray WM, Kepinski S, Rouse D, Leyser O, Estelle M (2001) Auxin regulates SCFTIR1-dependent degradation of AUX/IAA proteins. Nature 414: 271-276
Pubmed: Author and Title
CrossRef: Author and Title
Google Scholar: Author Only Title Only Author and Title

Halkier BA, Gershenzon J (2006) Biology and biochemistry of glucosinolates. Annu Rev Plant Biol 57: 303-333
Pubmed: Author and Title
CrossRef: Author and Title
Google Scholar: Author Only Title Only Author and Title

Hamann T, Benkova E, Baurle I, Kientz M, Jurgens G (2002) The Arabidopsis BODENLOS gene encodes an auxin response protein inhibiting MONOPTEROS-mediated embryo patterning. Gene Dev 16: 1610-1615
Pubmed: Author and Title
CrossRef: Author and Title
Google Scholar: Author Only Title Only Author and Title

He H, Liang G, Li Y, Wang F, Yu DQ (2014) Two Young MicroRNAs Originating from Target Duplication Mediate Nitrogen Starvation Adaptation via Regulation of Glucosinolate Synthesis in Arabidopsis thaliana. Plant Physiol 164: 853-865
Pubmed: Author and Title
CrossRef: Author and Title
Google Scholar: Author Only Title Only Author and Title

Iglesias MJ, Terrile MC, Bartoli CG, D'Ippolito S, Casalongue CA (2010) Auxin signaling participates in the adaptative response against oxidative stress and salinity by interacting with redox metabolism in Arabidopsis. Plant Mol Biol 74: 215-222
Pubmed: Author and Title
CrossRef: Author and Title
Google Scholar: Author Only Title Only Author and Title

Ji HT, Wang SF, Li KX, Szakonyi D, Koncz C, Li X (2015) PRL1 modulates root stem cell niche activity and meristem size through WOX5 and PLTs in Arabidopsis. Plant J 81: 399-412
Pubmed: Author and Title

CrossRef: Author and Title
Google Scholar: Author Only Title Only Author and Title

Katz E, Nisani S, Yadav BS, Woldemariam MG, Shai B, Obolski U, Ehrlich M, Shani E, Jander G, Chamovitz DA (2015) The glucosinolate breakdown product indole-3-carbinol acts as an auxin antagonist in roots of Arabidopsis thaliana. Plant J 82: 547-555
Pubmed: Author and Title
CrossRef: Author and Title
Google Scholar: Author Only Title Only Author and Title

Kovtun Y, Chiu WL, Tena G, Sheen J (2000) Functional analysis of oxidative stress-activated mitogen-activated protein kinase cascade in plants. Proc Natl Acad Sci USA 97: 2940-2945
Pubmed: Author and Title
CrossRef: Author and Title
Google Scholar: Author Only Title Only Author and Title

Kwak JM, Nguyen V, Schroeder JI (2006) The role of reactive oxygen species in hormonal responses. Plant Physiol 141: 323-329
Pubmed: Author and Title
CrossRef: Author and Title
Google Scholar: Author Only Title Only Author and Title

Laskowski M, Grieneisen VA, Hofhuis H, ten Hove CA, Hogeweg P, Maree AFM, Scheres B (2008) Root System Architecture from Coupling Cell Shape to Auxin Transport. Plos Biol 6: 2721-2735
Pubmed: Author and Title
CrossRef: Author and Title
Google Scholar: Author Only Title Only Author and Title

Li J, Xu HH, Liu WC, Zhang XW, Lu YT (2015) Ethylene Inhibits Root Elongation during Alkaline Stress through AUXIN1 and Associated Changes in Auxin Accumulation. Plant Physiol 168: 1777-1791
Pubmed: Author and Title
CrossRef: Author and Title
Google Scholar: Author Only Title Only Author and Title

Liu W, Li RJ, Han TT, Cai W, Fu ZW, Lu YT (2015) Salt Stress Reduces Root Meristem Size by Nitric Oxide-Mediated Modulation of Auxin Accumulation and Signaling in Arabidopsis. Plant Physiol 168: 343-U607
Pubmed: Author and Title
CrossRef: Author and Title
Google Scholar: Author Only Title Only Author and Title

Lombardo MC, Graziano M, Polacco JC, Lamattina L (2006) Nitric oxide functions as a positive regulator of root hair development. Plant Signal Behav 1: 28-33
Pubmed: Author and Title
CrossRef: Author and Title
Google Scholar: Author Only Title Only Author and Title

Nardi P, Akutsu M, Pariasca-Tanaka J, Wissuwa M (2013) Effect of methyl 3-4-hydroxyphenyl propionate, a Sorghum root exudate, on N dynamic, potential nitrification activity and abundance of ammonia-oxidizing bacteria and archaea. Plant Soil 367: 627-637
Pubmed: Author and Title
CrossRef: Author and Title
Google Scholar: Author Only Title Only Author and Title

Neal CS, Fredericks DP, Griffiths CA, Neale AD (2010) The characterisation of AOP2: a gene associated with the biosynthesis of aliphatic alkenyl glucosinolates in Arabidopsis thaliana. BMC Plant Biol 10
Pubmed: Author and Title
CrossRef: Author and Title
Google Scholar: Author Only Title Only Author and Title

Oono Y, Ooura C, Rahman A, Aspuria ET, Hayashi K, Tanaka A, Uchimiya H (2003) p-Chlorophenoxyisobutyric acid impairs auxin response in Arabidopsis root. Plant Physiol 133: 1135-1147
Pubmed: Author and Title
CrossRef: Author and Title
Google Scholar: Author Only Title Only Author and Title

Overvoorde P, Fukaki H, Beeckman T (2010) Auxin Control of Root Development. Cold Spring Harbor Perspectives In Biology 2
Pubmed: Author and Title
CrossRef: Author and Title
Google Scholar: Author Only Title Only Author and Title

Peret B, Swarup K, Ferguson A, Seth M, Yang YD, Dhondt S, James N, Casimiro I, Perry P, Syed A, Yang HB, Reemmer J, Venison E, Howells C, Perez-Amador MA, Yun JG, Alonso J, Beemster GTS, Laplaze L, Murphy A, Bennett MJ, Nielsen E, Swarup R (2012) AUX/LAX Genes Encode a Family of Auxin Influx Transporters That Perform Distinct Functions during Arabidopsis Development. Plant Cell 24: 2874-2885
Pubmed: Author and Title
CrossRef: Author and Title
Google Scholar: Author Only Title Only Author and Title

Rouse D, Mackay P, Stirnberg P, Estelle M, Leyser O (1998) Changes in auxin response from mutations in an AUX/IAA gene. Science 279: 1371-1373
Pubmed: Author and Title
CrossRef: Author and Title
Google Scholar: Author Only Title Only Author and Title

Sabatini S, Beis D, Wolkenfelt H, Murfett J, Guilfoyle T, Malamy J, Benfey P, Leyser O, Bechtold N, Weisbeek P, Scheres B (1999) An auxin-dependent distal organizer of pattern and polarity in the Arabidopsis root. Cell 99: 463-472
Pubmed: Author and Title
CrossRef: Author and Title
Google Scholar: Author Only Title Only Author and Title

Sanz L, Fernandez-Marcos M, Modrego A, Lewis DR, Muday GK, Pollmann S, Duenas M, Santos-Buelga C, Lorenzo O (2014) Nitric oxide plays a role in stem cell niche homeostasis through its interaction with auxin. Plant Physiol 166: 1972-1984
Pubmed: Author and Title
CrossRef: Author and Title
Google Scholar: Author Only Title Only Author and Title

Schlesinger WH (2009) On the fate of anthropogenic nitrogen. Proc Natl Acad Sci USA 106: 203-208
Pubmed: Author and Title
CrossRef: Author and Title
Google Scholar: Author Only Title Only Author and Title

Shroff R, Vergara F, Muck A, Svatos A, Gershenzon J (2008) Nonuniform distribution of glucosinolates in Arabidopsis thaliana leaves has important consequences for plant defense. Proc Natl Acad Sci USA 105: 6196-6201
Pubmed: Author and Title
CrossRef: Author and Title
Google Scholar: Author Only Title Only Author and Title

Spitzner A, Perzlmaier AF, Geillinger KE, Reihl P, Stolz J (2008) The proline-dependent transcription factor Put3 regulates the expression of the riboflavin transporter MCH5 in Saccharomyces cerevisiae. Genetics 180: 2007-2017
Pubmed: Author and Title
CrossRef: Author and Title
Google Scholar: Author Only Title Only Author and Title

Subbarao GV, Nakahara K, Ishikawa T, Ono H, Yoshida M, Yoshihashi T, Zhu YY, Zakir HAKM, Deshpande SP, Hash CT, Sahrawat KL (2013) Biological nitrification inhibition (BNI) activity in sorghum and its characterization. Plant Soil 366: 243-259
Pubmed: Author and Title
CrossRef: Author and Title
Google Scholar: Author Only Title Only Author and Title

Swarup R, Perry P, Hagenbeek D, Van Der Straeten D, Beemster GTS, Sandberg G, Bhalerao R, Ljung K, Bennett MJ (2007) Ethylene upregulates auxin biosynthesis in Arabidopsis seedlings to enhance inhibition of root cell elongation. Plant Cell 19: 2186-2196
Pubmed: Author and Title
CrossRef: Author and Title
Google Scholar: Author Only Title Only Author and Title

Terrile MC, Paris R, Calderon-Villalobos LIA, Iglesias MJ, Lamattina L, Estelle M, Casalongue CA (2012) Nitric oxide influences auxin signaling through S-nitrosylation of the Arabidopsis TRANSPORT INHIBITOR RESPONSE 1 auxin receptor. Plant J 70: 492-500
Pubmed: Author and Title
CrossRef: Author and Title
Google Scholar: Author Only Title Only Author and Title

Tewari RK, Kim S, Hahn EJ, Paek KY (2008) Involvement of nitric oxide-induced NADPH oxidase in adventitious root growth and antioxidant defense in Panax ginseng. Plant Biotechnol Rep 2: 113-122
Pubmed: Author and Title
CrossRef: Author and Title
Google Scholar: Author Only Title Only Author and Title

Tong Y, Gabriel-Neumann E, Krumbein A, Ngwene B, George E, Schreiner M (2015) Interactive effects of arbuscular mycorrhizal fungi and intercropping with sesame (Sesamum indicum) on the glucosinolate profile in broccoli (Brassica oleracea var. Italica). Environ Exp Bot 109: 288-295
Pubmed: Author and Title
CrossRef: Author and Title
Google Scholar: Author Only Title Only Author and Title

Tsukagoshi H, Busch W, Benfey PN (2010) Transcriptional Regulation of ROS Controls Transition from Proliferation to Differentiation in the Root. Cell 143: 606-616
Pubmed: Author and Title
CrossRef: Author and Title
Google Scholar: Author Only Title Only Author and Title

Ulmasov T, Murfett J, Hagen G, Guilfoyle TJ (1997) Aux/IAA proteins repress expression of reporter genes containing natural and highly active synthetic auxin response elements. Plant Cell 9: 1963-1971
Pubmed: Author and Title
CrossRef: Author and Title
Google Scholar: Author Only Title Only Author and Title

van Dam NM, Witjes L, Svatos A (2004) Interactions between aboveground and belowground induction of glucosinolates in two wild Brassica species. New Phytol 161: 801-810
Pubmed: Author and Title
CrossRef: Author and Title
Google Scholar: Author Only Title Only Author and Title

Van de Poel B, Smet D, Van der Straeten D (2015) Ethylene and Hormonal Cross Talk in Vegetative Growth and Development. Plant Physiol 169: 61-72
Pubmed: Author and Title
CrossRef: Author and Title
Google Scholar: Author Only Title Only Author and Title

Wang D, Pajerowska-Mukhtar K, Culler AH, Dong XN (2007) Salicylic acid inhibits pathogen growth in plants through repression of the auxin signaling pathway. Curr Biol 17: 1784-1790
Pubmed: Author and Title
CrossRef: Author and Title
Google Scholar: Author Only Title Only Author and Title

Wang L, Guo YJ, Jia LX, Chu HY, Zhou S, Chen KM, Wu D, Zhao LQ (2014) Hydrogen Peroxide Acts Upstream of Nitric Oxide in the Heat Shock Pathway in Arabidopsis Seedlings. Plant Physiol 164: 2184-2196
Pubmed: Author and Title
CrossRef: Author and Title
Google Scholar: Author Only Title Only Author and Title

Wang YN, Li KX, Li X (2009) Auxin redistribution modulates plastic development of root system architecture under salt stress in Arabidopsis thaliana. J Plant Physiol 166: 1637-1645
Pubmed: Author and Title
CrossRef: Author and Title
Google Scholar: Author Only Title Only Author and Title

Wink DA, Mitchell JB (1998) Chemical biology of nitric oxide: Insights into regulatory, cytotoxic, and cytoprotective mechanisms of nitric oxide. Free Radic Biol Med 25: 434-456
Pubmed: Author and Title
CrossRef: Author and Title
Google Scholar: Author Only Title Only Author and Title

Xu J, Yin H, Li Y, Liu X (2010a) Nitric oxide is associated with long-term zinc tolerance in Solanum nigrum. Plant Physiol 154: 1319-1334
Pubmed: Author and Title
CrossRef: Author and Title
Google Scholar: Author Only Title Only Author and Title

Xu J, Yin HX, Liu X, Li X (2010b) Salt affects plant Cd-stress responses by modulating growth and Cd accumulation. Planta 231: 449-459
Pubmed: Author and Title
CrossRef: Author and Title
Google Scholar: Author Only Title Only Author and Title

Xu J, Zhu Y, Ge Q, Li Y, Sun J, Zhang Y, Liu X (2012) Comparative physiological responses of Solanum nigrum and Solanum torvum to cadmium stress. New Phytol 196: 125-138
Pubmed: Author and Title
CrossRef: Author and Title
Google Scholar: Author Only Title Only Author and Title

Yuan HM, Xu HH, Liu WC, Lu YT (2013) Copper Regulates Primary Root Elongation Through PIN1-Mediated Auxin Redistribution. Plant Cell Physiol 54: 766-778
Pubmed: Author and Title
CrossRef: Author and Title
Google Scholar: Author Only Title Only Author and Title

Yuan HM, Huang X (2016) Inhibition of root meristem growth by cadmium involves nitric oxide-mediated repression of auxin accumulation and signalling in Arabidopsis. Plant Cell Environ 39: 120-135
Pubmed: Author and Title
CrossRef: Author and Title
Google Scholar: Author Only Title Only Author and Title

Yuan TT, Xu HH, Zhang KX, Guo TT, Lu YT (2014) Glucose inhibits root meristem growth via ABA INSENSITIVE 5, which represses PIN1 accumulation and auxin activity in Arabidopsis. Plant Cell Environ 37: 1338-1350
Pubmed: Author and Title
CrossRef: Author and Title
Google Scholar: Author Only Title Only Author and Title

Zakir HA, Subbarao GV, Pearse SJ, Gopalakrishnan S, Ito O, Ishikawa T, Kawano N, Nakahara K, Yoshihashi T, Ono H, Yoshida M (2008) Detection, isolation and characterization of a root-exuded compound, methyl 3-(4-hydroxyphenyl) propionate, responsible for biological nitrification inhibition by sorghum (Sorghum bicolor). New Phytol 180: 442-451
Pubmed: Author and Title
CrossRef: Author and Title
Google Scholar: Author Only Title Only Author and Title

Zhang H, Jennings A, Barlow PW, Forde BG (1999) Dual pathways for regulation of root branching by nitrate. Proc Natl Acad Sci USA 96: 6529-6534
Pubmed: Author and Title
CrossRef: Author and Title
Google Scholar: Author Only Title Only Author and Title

Zhao Y, Christensen SK, Fankhauser C, Cashman JR, Cohen JD,Weigel D, Chory J (2001) A role for flavin monooxygenaselike

enzymes in auxin biosynthesis. Science 291: 306-309
Pubmed: Author and Title
CrossRef: Author and Title
Google Scholar: Author Only Title Only Author and Title

Zheng BL, Chen XM, McCormick S (2011) The Anaphase-Promoting Complex Is a Dual Integrator That Regulates Both MicroRNA-Mediated Transcriptional Regulation of Cyclin B1 and Degradation of Cyclin B1 during Arabidopsis Male Gametophyte Development. Plant Cell 23: 1033-1046
Pubmed: Author and Title
CrossRef: Author and Title
Google Scholar: Author Only Title Only Author and Title

Supporting Information

Tab. S1 Differential expression gene involved in glucosinolate biosynthesis by RNA-seq analysis.

	MHPP40/ck		MHPP80/ck		gene annotation
	log2FC	**FDR**	**log2FC**	**FDR**	
Glucosinolate biosynthesis					
AT1G16400	1.708240112	5.55112E-16	2.306720135	0	CYP79F2
AT1G16410	3.631987707	0	4.000006147	0	BUS1, BUSHY 1, CYP79F1, CYTOCHROME P450 79F1, SPS1
AT3G19710	2.277628273	0	2.843176917	0	BCAT4
AT4G13770	1.918104411	0	2.339267801	0	CYP83A1, REF2
AT5G23010	1.880659295	0	2.016787262	0	MAM1, IMS3
AT5G23020	1.509774991	0	1.778715553	0	IMS2, MAM-L, MAM3
AT1G24100	-	-	1.006089374	4.4E-06	UGT74B1
AT2G20610	-	-	1.342807875	6.13E-11	ALF1, HLS3, HOOKLESS 3, ROOTY, ROOTY 1, RTY, RTY1, SUR1
AT1G10070	-	-	-2.119278741	1.34E-09	ATBCAT-2
tryptophan, Valine, leucine and isoleucine biosynthesis					
AT1G52410	1.2851172	5.43682E-07	1.184226949	6.19E-05	TSK-ASSOCIATING PROTEIN 1
AT2G43100	1.988853584	0	2.320658481	0	ISOPROPYLMALATE ISOMERASE 2
AT3G58990	2.286122899	0	2.675974164	0	ISOPROPYLMALATE ISOMERASE 1
AT5G14200	1.768110263	0	2.089694591	0	ISOPROPYLMALATE DEHYDROGENASE 1

Table S2. List of the primers for qRT-PCR analysis of the genes.

Gene	Primers
AtASA1	5'ATGTCTTCCTCTATGAACGTAGC3' 5'ACAGCGGTAAATTGGTATAAGG3'
AtPAT1	5'ATGGTTATTGCGGTGGCGAC3' 5'ATCGTCGCCGACTCAATGTC3'
AtAMI1	5'CGGACTTACTCCAATGGCTCAG3' 5'GCTGCTGCAGGAGAACGCAACC3'
AtSUR1	5'GACCACCAAGGTGTTACAATCC3' 5'ATTATTGTGGCAGGGTCAGG3'
AtTAA1	5'CTCCAAGATCACAGGCCACGCTGGG3' 5'GACTCCTTAGACACACCAATCGAGTTC3'
AtYUC2	5'GGTGACACGGATCGGTTAGGGT3' 5'TGCCGAATAATGCATTACCCGT3'
AtYUC3	5'CTTGAGATTGATTCCGTTATTC3 5'GGAGAAGAAGTCGTTGTC3'
AtYUC9	5'ATCTTGCTAACCACAATG3' 5'CCACTTCATCATCATCAC3
AtAAO1	5'TGCCTGTTCCAGCAACAATG3' 5'TAAGCAGAACACCGCCATTG 3'
AtAAO3	5'GGAGTCAGCGAGGTGGAAGT3' 5'TGCTCCTTCGGTCTGTCCTAA3'
AtAUX1	5'TCACGCGGTTACTGTTGAGA3' 5'TTGGAGTGGTCGAGAAGTGC3'
AtPIN1	5'ACGGCTGCTGGAACTGCTGC3' 5'CGTACTGGTTGTCGTTACTATT3'
AtPIN2	5'TATATTCGGAATGCTGGTTGCTTTG3' 5'CCATACACCTAAGCCTGACCTGGAA3'

AtPIN4	5’GTTGTCTCTGATCAACCTCGAAA3’ 5’TATCAAGACCGCCGATATCATC3’
AtPIN7	5’CCAAGATTAGTGGAACGCAAC3’ 5’GAAAAGGGTTTTTGGATCCTC3’
AtCYP79F2	5’AAGCTCAATGCGTCGAATTTTGT3’ 5’GGCAACATGAGGTGGGACA3’
AtCYP79F1	5’TCCCAAAGGTAGCCACATTCA3’ 5’ACGCATCTCTGTTTCCACCA3’
AtBCAT4	5’TCCTGTGAGTGTTTCGGATGA3’ 5’TACTGAAGAACAGCAGCGCA3’
AtCYP83A1	5’AGAGAGTCAAGCCCGAAACC3’ 5’CCCGCCACTACAATATCCAAGA3’
AtMAM1	5’ACATTGAGGCGACTTGGGAG3’ 5’AAATCCTTGTCCGACCTGCC3’
AtMAM3	5’CTTGGAAAGCTTAGCGGACG3’ 5’TTTCAGCACCGTTCACCACT3’
AtTSA1	5’CTGCAGTCCAGGGAACAGAG3’ 5’TAAGCCGCGAAGCTCATTCA3’
AtIPMI2	5’AACCAGCAAGAGCGTGATGA3’ 5’TCGCCGCCGATTATGATTGA3’
AtIPMI1	5’CTCAAGTCCGCCTCCACAAT3’ 5’GATGAGAGTGCCGTACTCGG3’
AtIMD1	5’ TGGGATGCAAGGAAATGGGT3’ 5’AGGCAGGAGACCTGTCAAATG3’

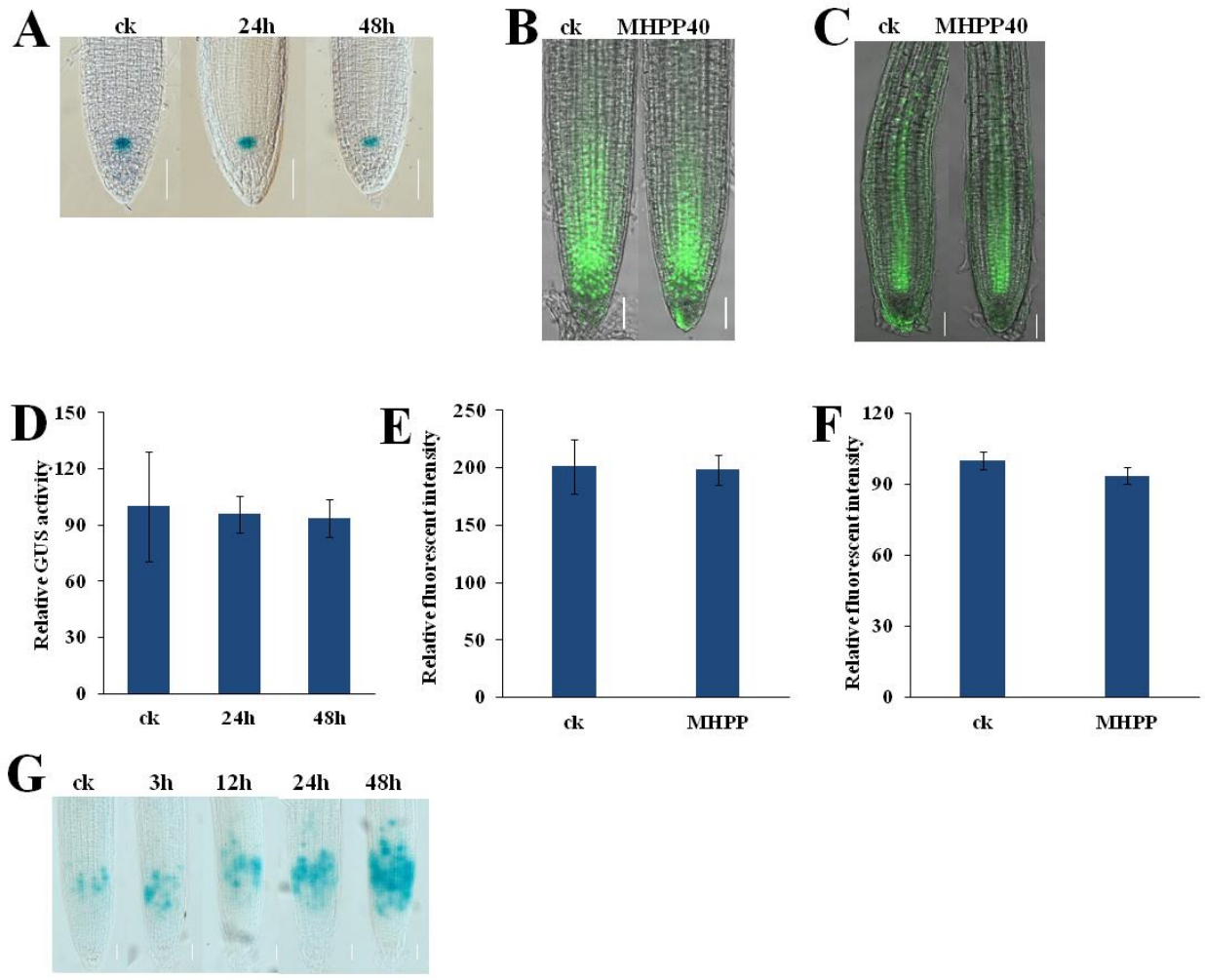

Fig. S1 Effects of MHPP on root meristem development. (A,D) Image of GUS staining of 5-d-old *QC25:GUS* seedlings exposed to 40 μM MHPP for 24 or 48 h (A) and the relative GUS activity of *QC25:GUS* seedlings (D) treated as in (A). Bars, 50 μm. The level of GUS activity in untreated roots was set to 100. (B,C,E,F) GFP fluorescence in the roots of 5-d-old *PLT1:GFP* (B) and *SHR:GFP* (C) seedlings exposed to 40 μM MHPP for 24 h and quantification of the *PLT1:GFP* (E) and *SHR:GFP* (F) fluorescence intensities in plants treated as in (B) and (C), respectively. Bars, 50 μm. The fluorescence intensity of untreated roots was set to 100. The error bars represent the SEM. The asterisks indicate significant differences with respect to the corresponding control ($P<0.01$ based on Tukey's test). (G) Image of GUS staining of 5-d-old *CYCB1;1:GUS* seedlings exposed to 80 μM MHPP for 3-48 h.

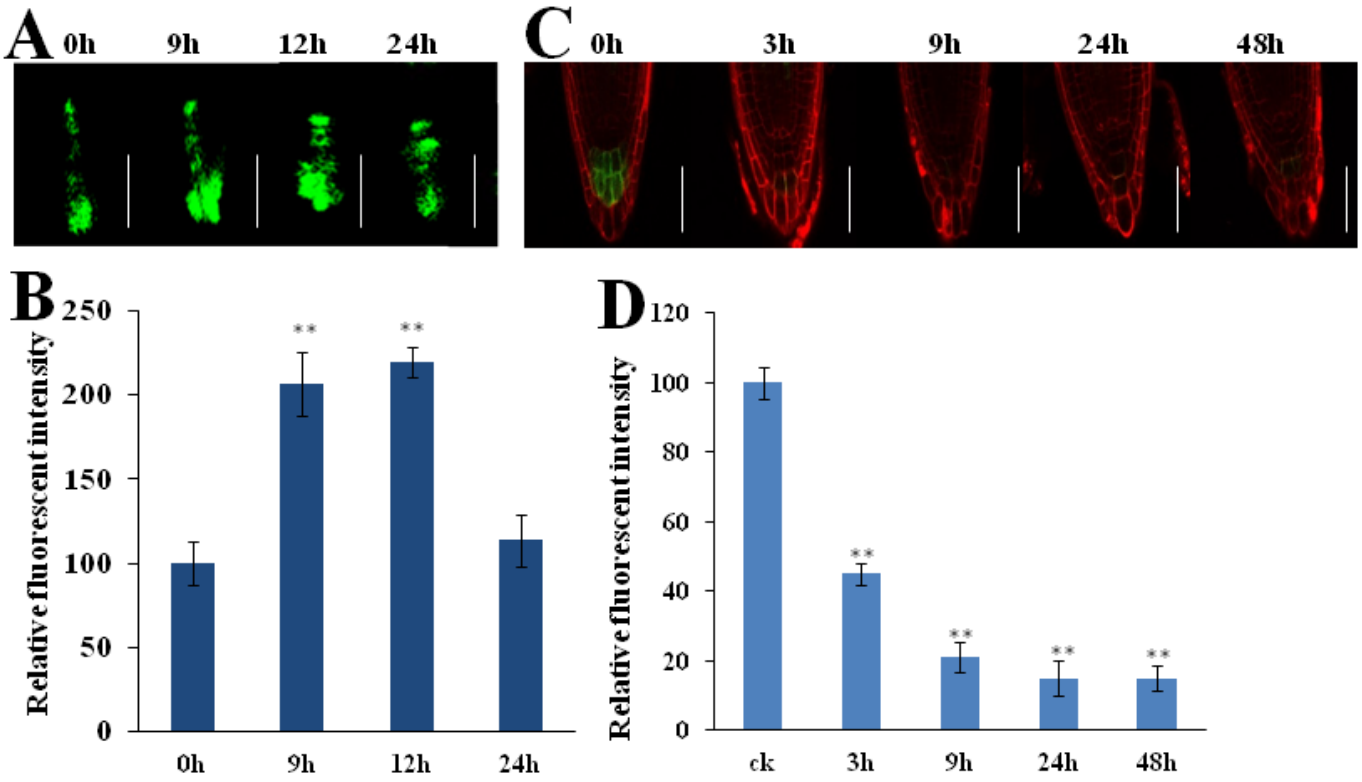

Fig. S2 GFP fluorescence in the roots of 5-d-old *DR5:GFP* (A) or *PIN4:GFP* (C) seedlings exposed to 80 μM MHPP for up to 48 h and quantification of *DR5:GFP* (B) or *PIN4:GFP* (D) fluorescence intensity in plants treated as in (A) and (C), respectively. The fluorescence intensity of untreated roots was set to 100. Bars, 50 μm. The error bars represent the SEM. The asterisks (**) indicate significant differences with respect to the corresponding control ($P<0.01$ based on Tukey's test).

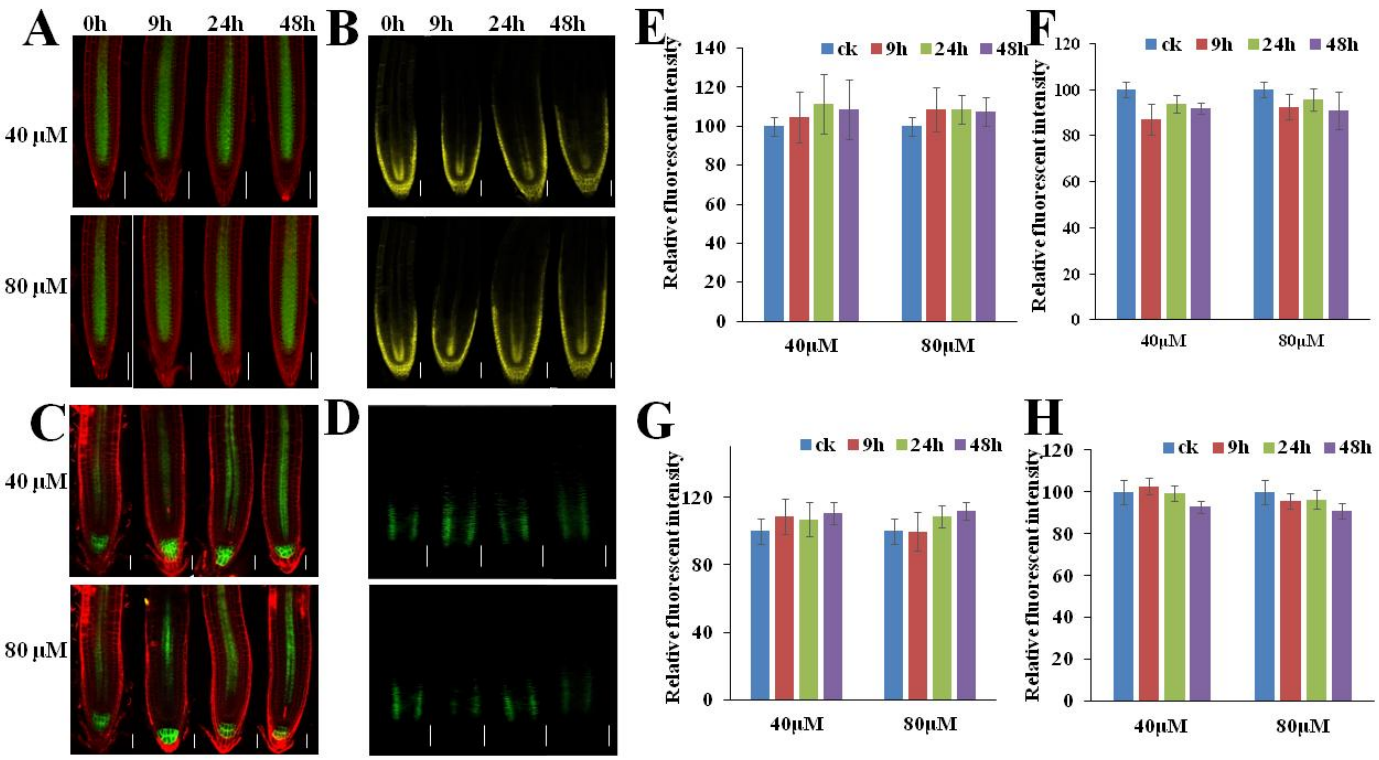

Fig. S3 GFP or YFP fluorescence in the roots of 5-d-old *PIN1:GFP* (A), *AUX1:YFP* (B), *PIN7:GFP* (C) or *PIN2:GFP* (D) seedlings exposed to 40 or 80 μM MHPP for up to 48 h and quantification of *PIN1:GFP* (E), *AUX1:YFP* (F), *PIN7:GFP* (G) or *PIN2:GFP* (H) fluorescence intensity in plants treated as in (A), (B), (C) and (D), respectively. The fluorescence intensity of untreated roots was set to 100. Bars, 50 μm. The error bars represent the SEM. The asterisks (**) indicate significant differences with respect to the corresponding control ($P<0.01$ based on Tukey's test).

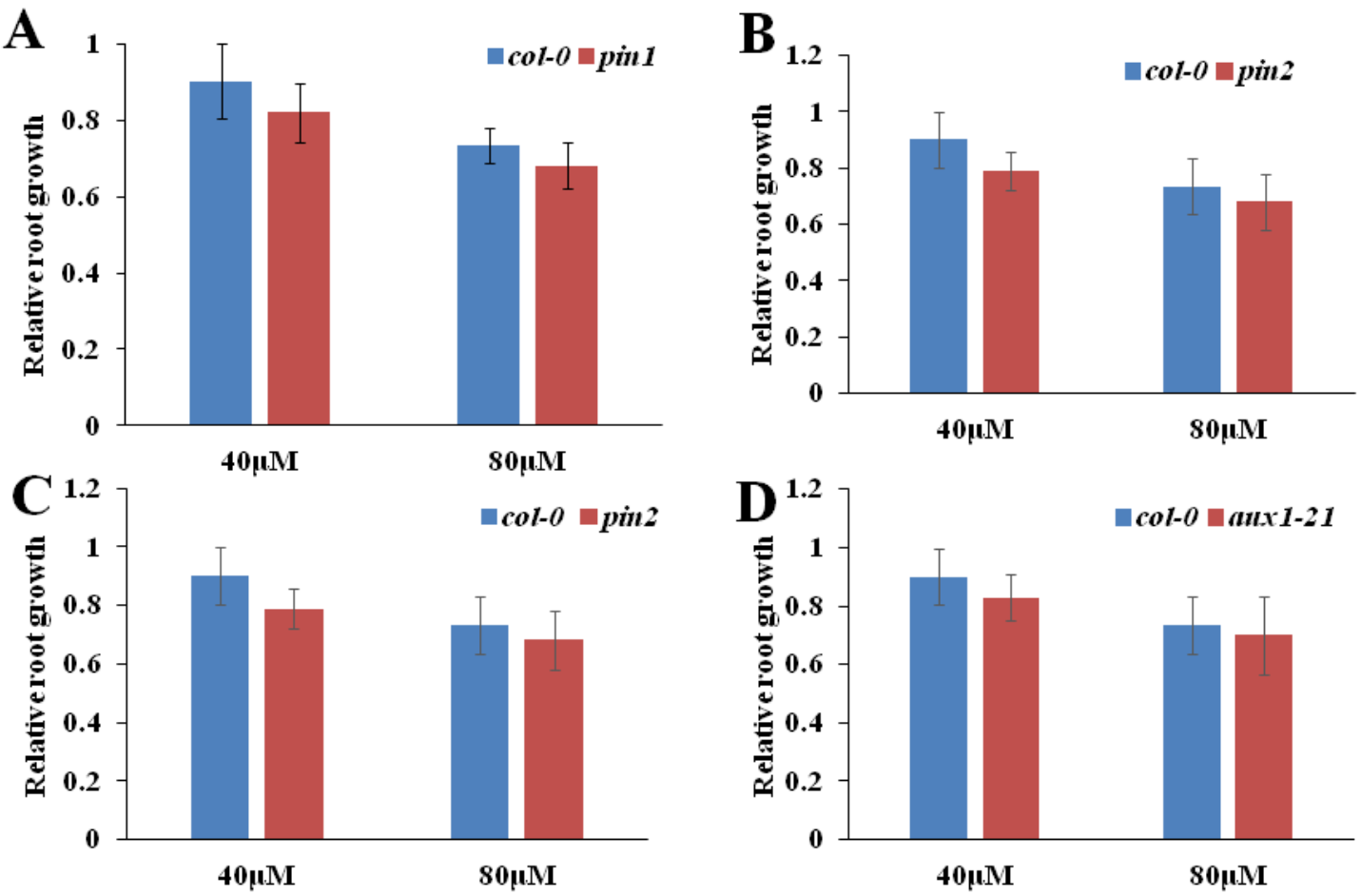

Fig. S4 Relative root growth of *col-0*, *pin1* (A), *pin2* (B), *pin7-2* (C), and *aux1-21* (D) seedlings treated with or without MHPP (40 μM or 80 μM) for 5 d. The lengths of untreated roots of *col-0*, *pin1*, *pin2*, *pin7-2*, and *aux1-21* plants were set to 1. The error bars represent the SEM. The asterisks indicate significant differences with respect to the corresponding control ($P<0.05$ based on Tukey's test).

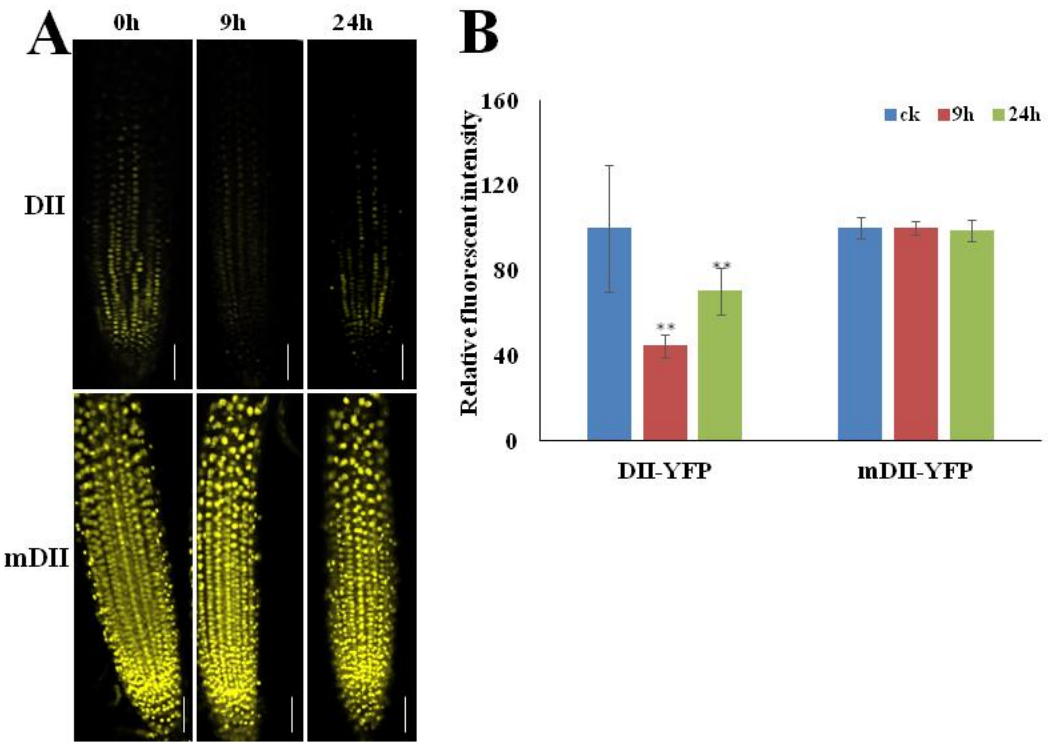

Fig. S5 YFP fluorescence in the roots of 5-d-old *DII-VENUS* or *mDII-VENUS* seedlings exposed to 80 μM MHPP for up to 24 h (A) and quantification of the *DII-VENUS* or *mDII-VENUS* (B) fluorescence intensity in plants treated as in (A). The fluorescence intensity of untreated roots was set to 100. Bars, 50 μm. The error bars represent the SEM. The asterisks (**) indicate significant differences with respect to the corresponding control ($P<0.01$ based on Tukey's test).

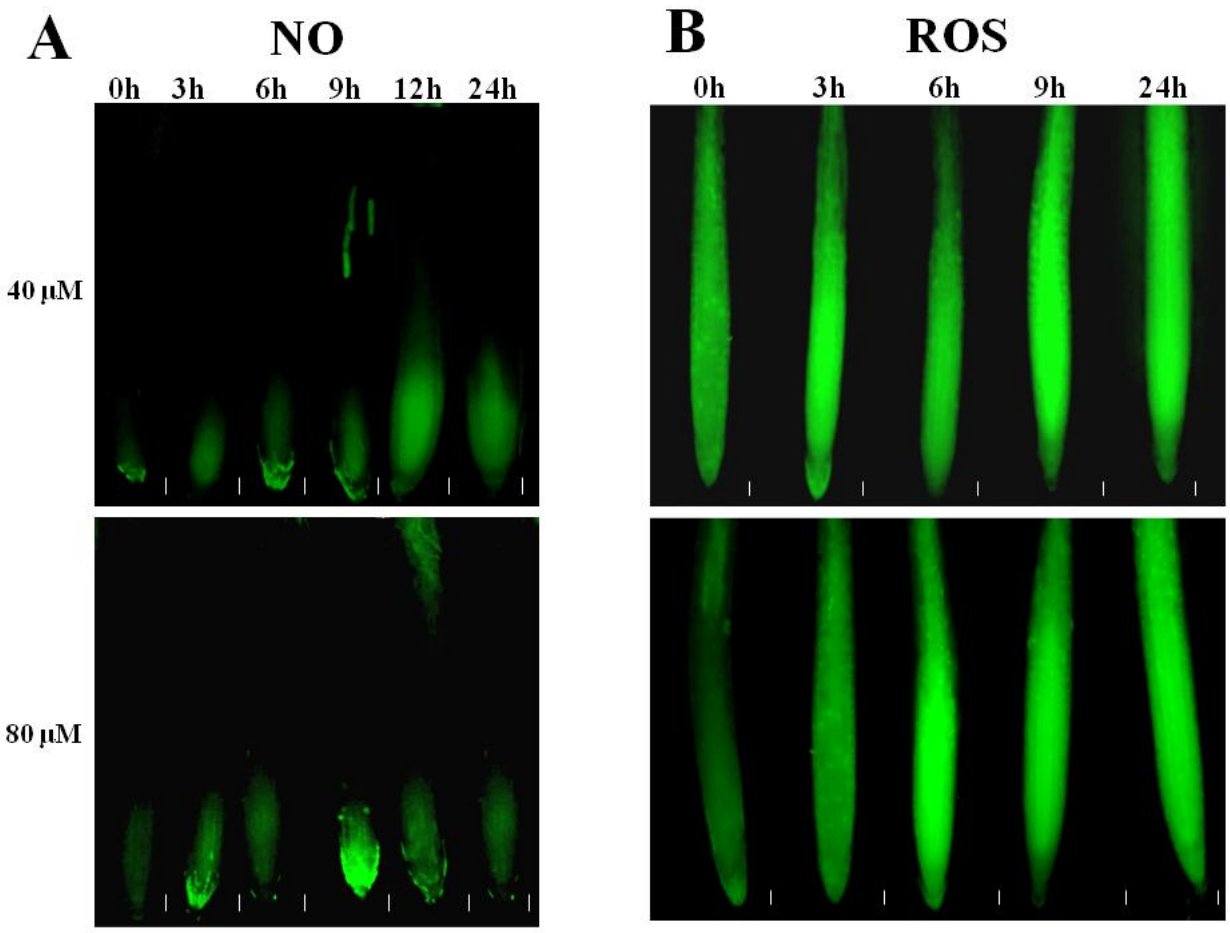

Fig. S6 Detection of NO (A) and ROS (B) production in the roots of 5-d-old wild-type seedlings exposed to 40 or 80 μM MHPP for up to 24 h using the NO-specific fluorescent probe DAF-2 DA and the ROS-specific fluorescent probe DCFH-DA, respectively. Bars, 50 μm.

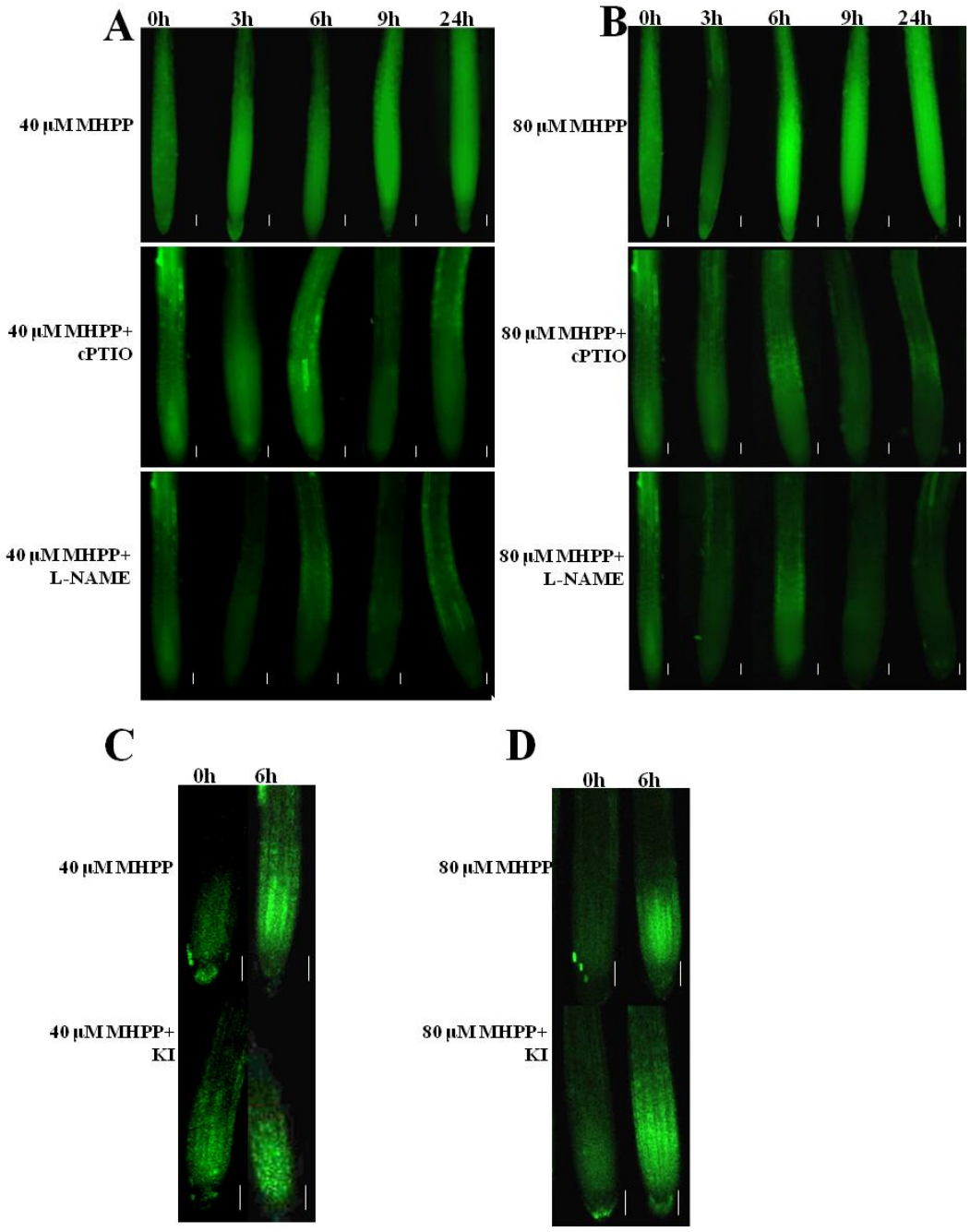

Fig. S7 (A,B) Detection of ROS production in the roots of 5-d-old wild-type seedlings exposed to 40 μM MHPP (A) or 80 μM MHPP (B) in the presence or absence of 200 μM cPTIO or 500 μM L-NAME for up to 24 h using the ROS-specific fluorescent probe DCFH-DA. (C,D) Detection of NO production in the roots of 5-d-old wild-type seedlings exposed to 40 μM MHPP (C) or 80 μM MHPP (D) in the presence or absence of 1 mM KI for 6 h using the NO-specific fluorescent probe DAF-2 DA. Bars, 50 μm.

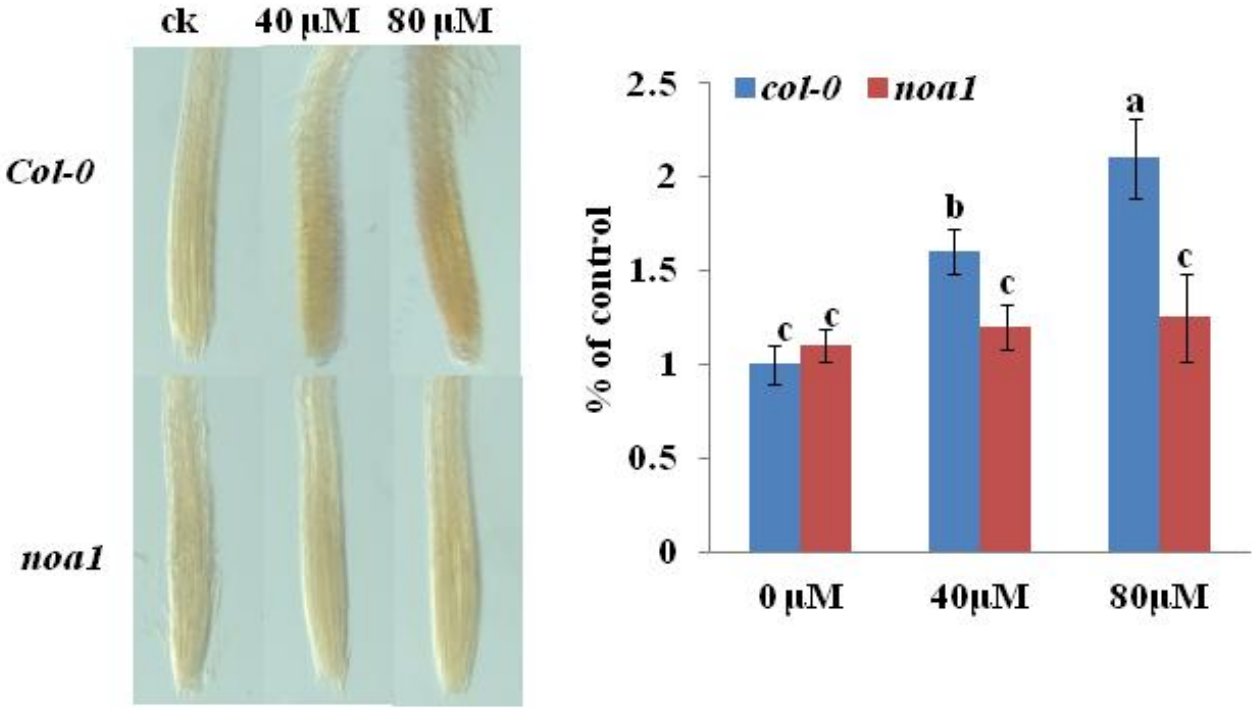

Fig. S8 Image of DAB staining of 5-d-old *col-0* or *noa1* seedlings exposed to 40 μM or 80 μM MHPP for 24 h. Bars, 50 μm.

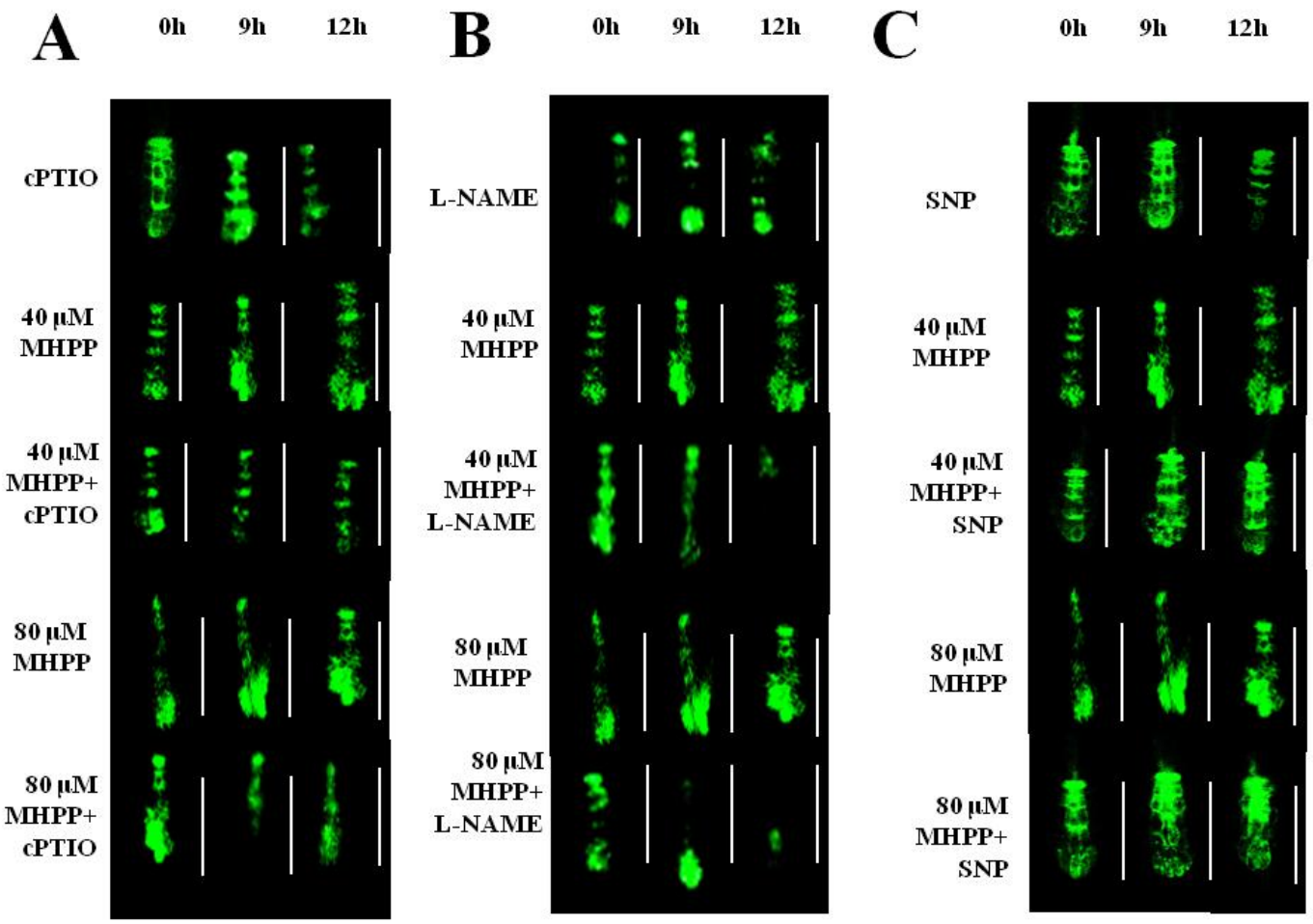

Fig. S9 GFP fluorescence in the roots of 5-d-old *DR5:GFP* seedlings exposed to 40 or 80 μM MHPP in the presence or absence of 200 μM cPTIO (A), 500 μM L-NAME (B) or 100 μM SNP (C) for 9 or 12 h. Bars, 50 μm.

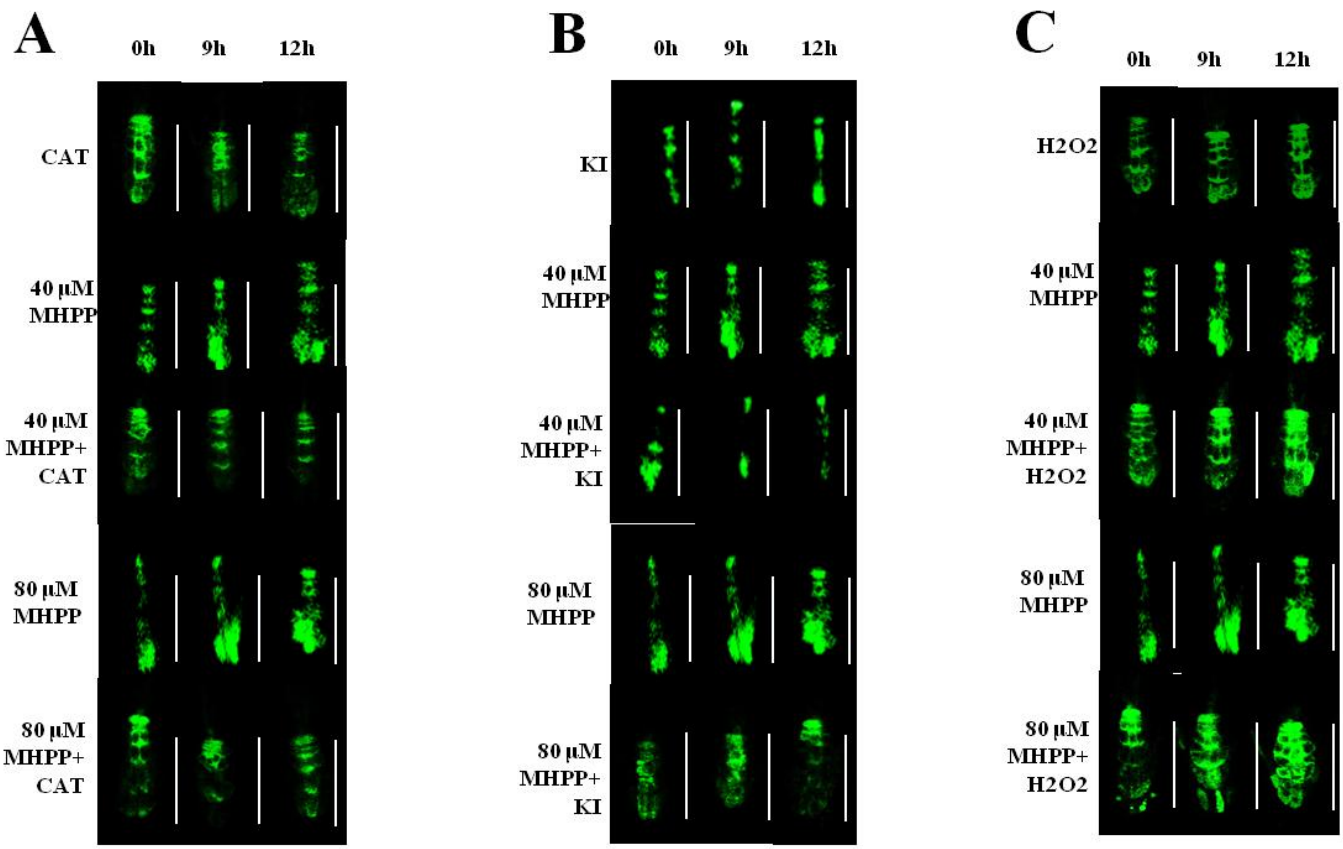

Fig. S10 GFP fluorescence in the roots of 5-d-old *DR5:GFP* seedlings exposed to 40 or 80 μM MHPP in the presence or absence of 200 μM CAT (A), 1 mM KI (B) or 500 μM H_2O_2 (C) for 9 or 12 h. Bars, 50 μm.

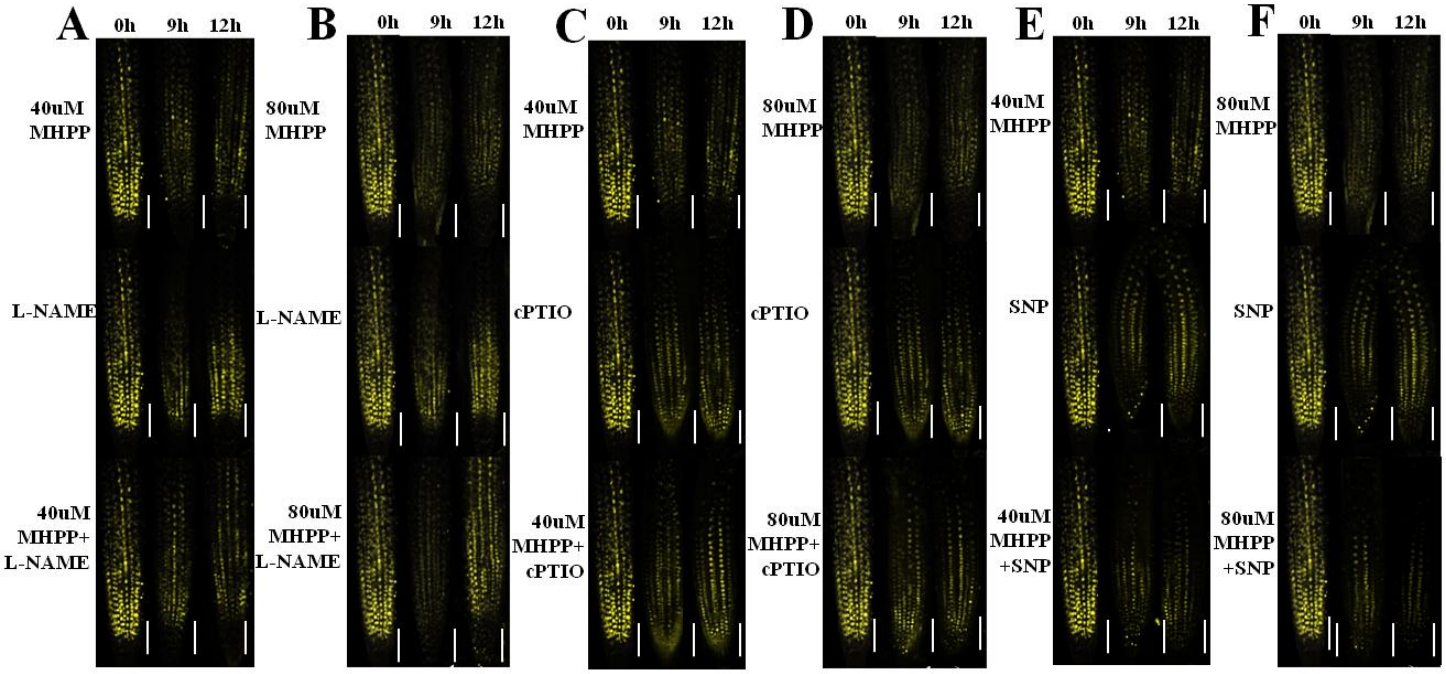

Fig. S11 YFP fluorescence in the roots of 5-d-old *DII-VENUS* seedlings exposed to 40 (A, C, E) or 80 μM (B, D, F) MHPP in the presence or absence of 500 μM L-NAME (A, B), 200 μM cPTIO (C, D), or 100 μM SNP (E, F) for 9 or 12 h. Bars, 50 μm.

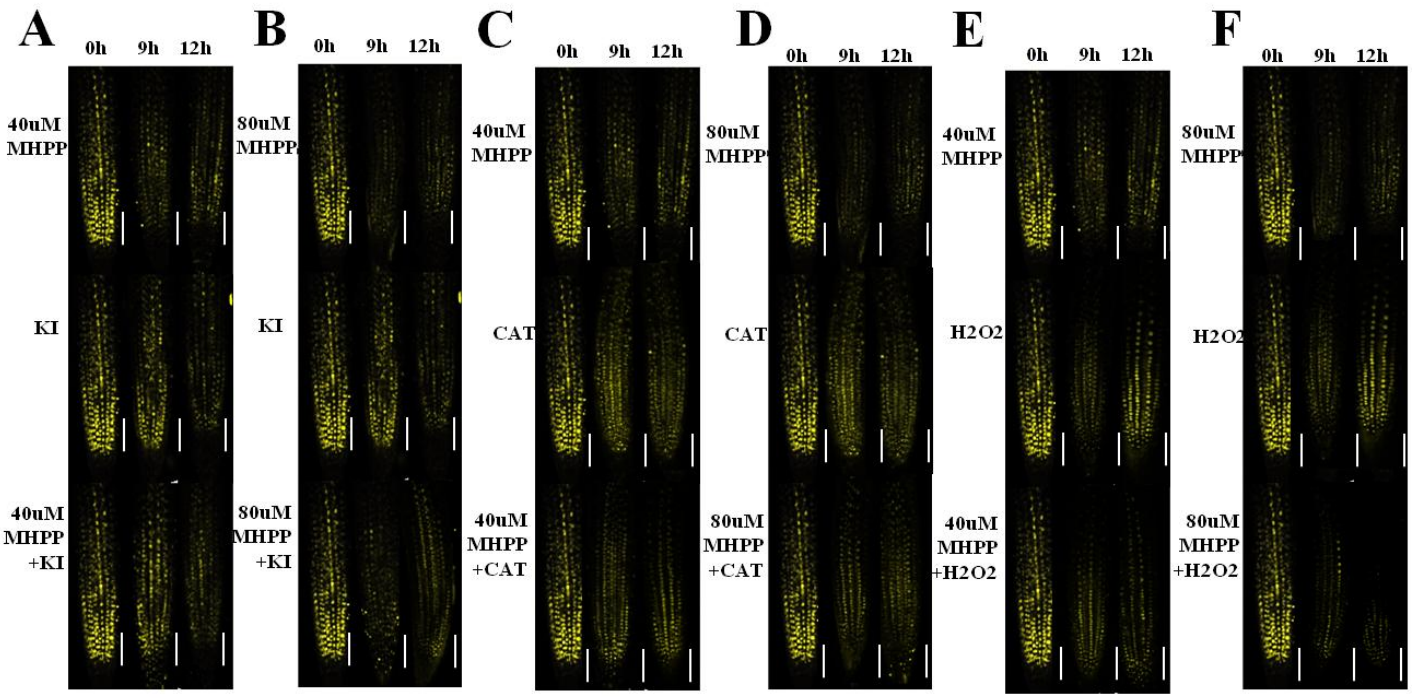

Fig. S12 YFP fluorescence in the roots of 5-d-old *DII-VENUS* seedlings exposed to 40 μM (A, C, E) or 80 μM (B, D, F) MHPP in the presence or absence of 1 mM (A, B), 200 μM CAT (C, D), or 500 μM H_2O_2 (E, F) for 9 or 12 h. Bars, 50 μm.

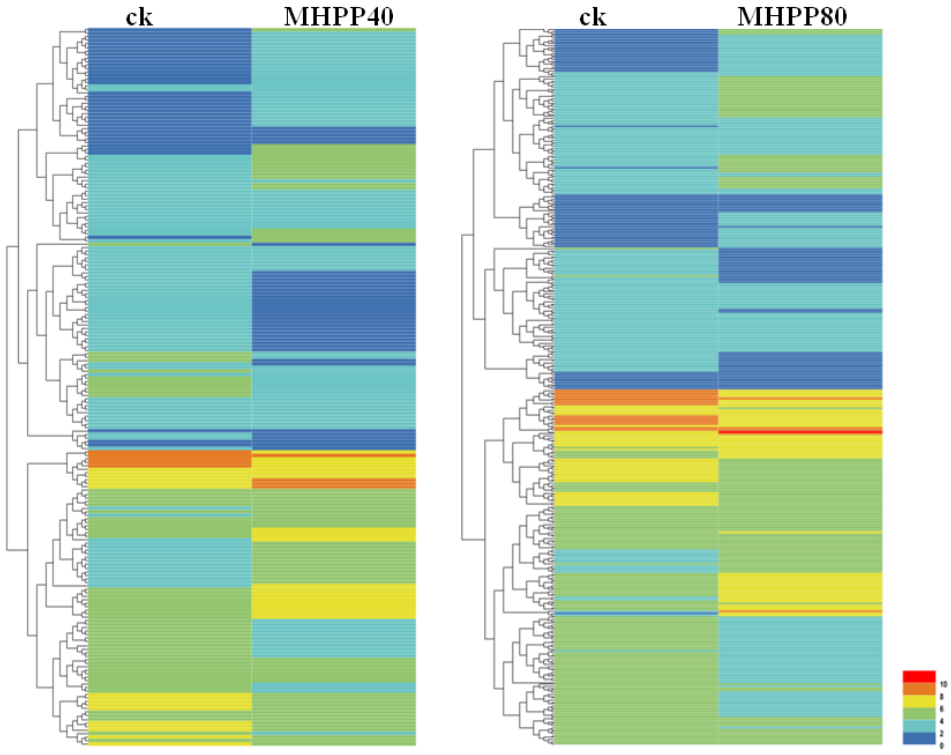

Fig. S13 Hierarchical clustering analysis of the differentially expressed genes in *Arabidopsis* roots treated with 40 or 80 μM MHPP for 2 d.

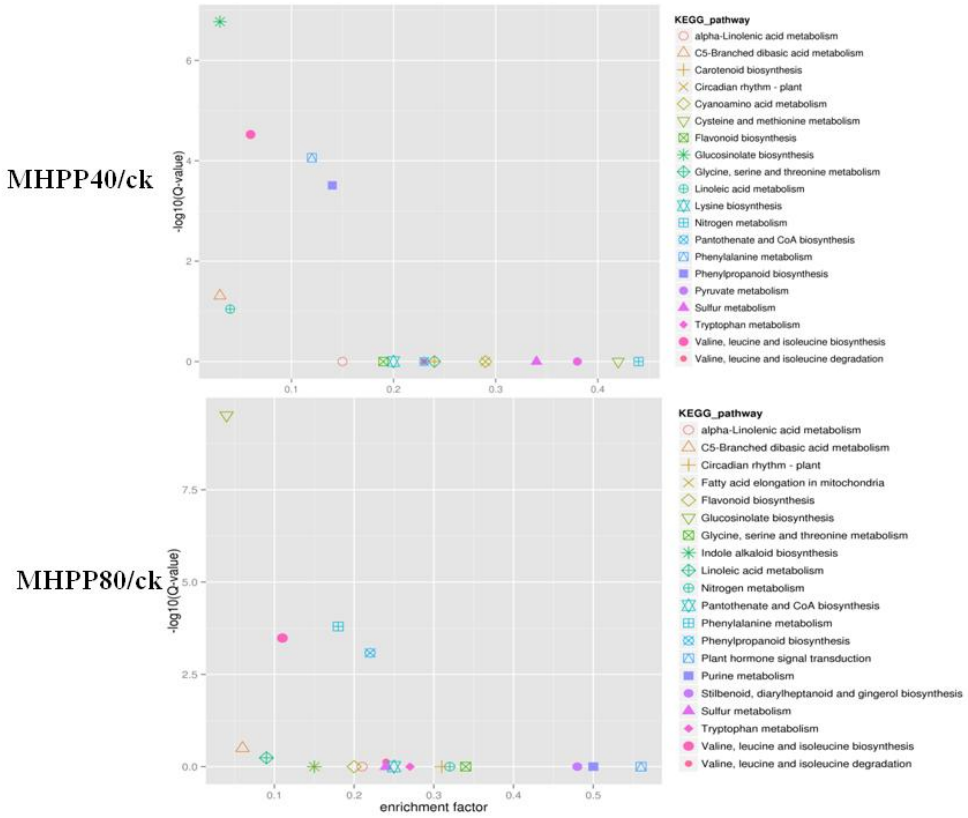

Fig. S14 KEGG pathway enrichment analysis of the differentially expressed genes in *Arabidopsis* roots treated with 40 or 80 μM MHPP for 2 d. The lower the enrichment factor, the more significant the enrichment of the pathway. The higher the -log10 value (Q-value), the greater the reliability of the significant enrichment.

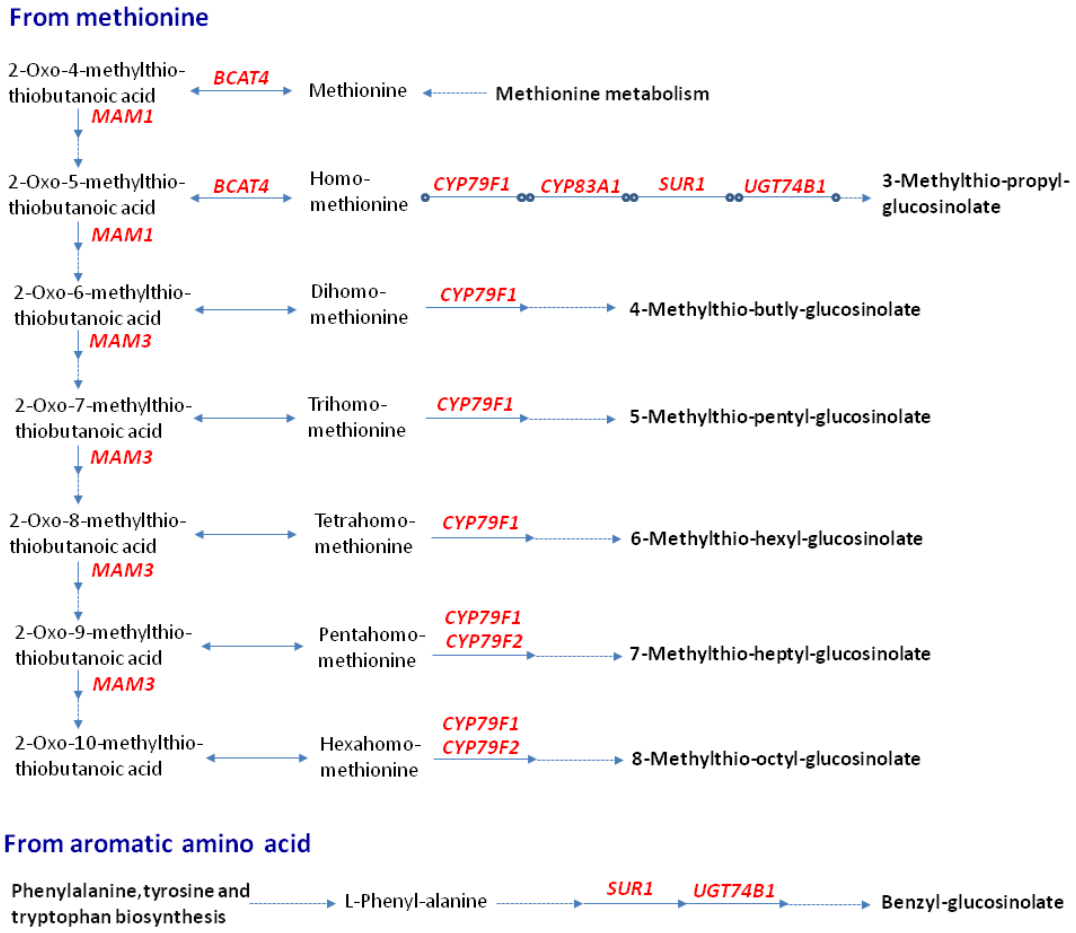

Fig. S15 Modulation of glucosinolate biosynthesis after MHPP treatment. The schematic representation was designed based on the results of RNA-seq and qRT-PCR analysis. The red italics represent up-regulated genes under MHPP treatment.

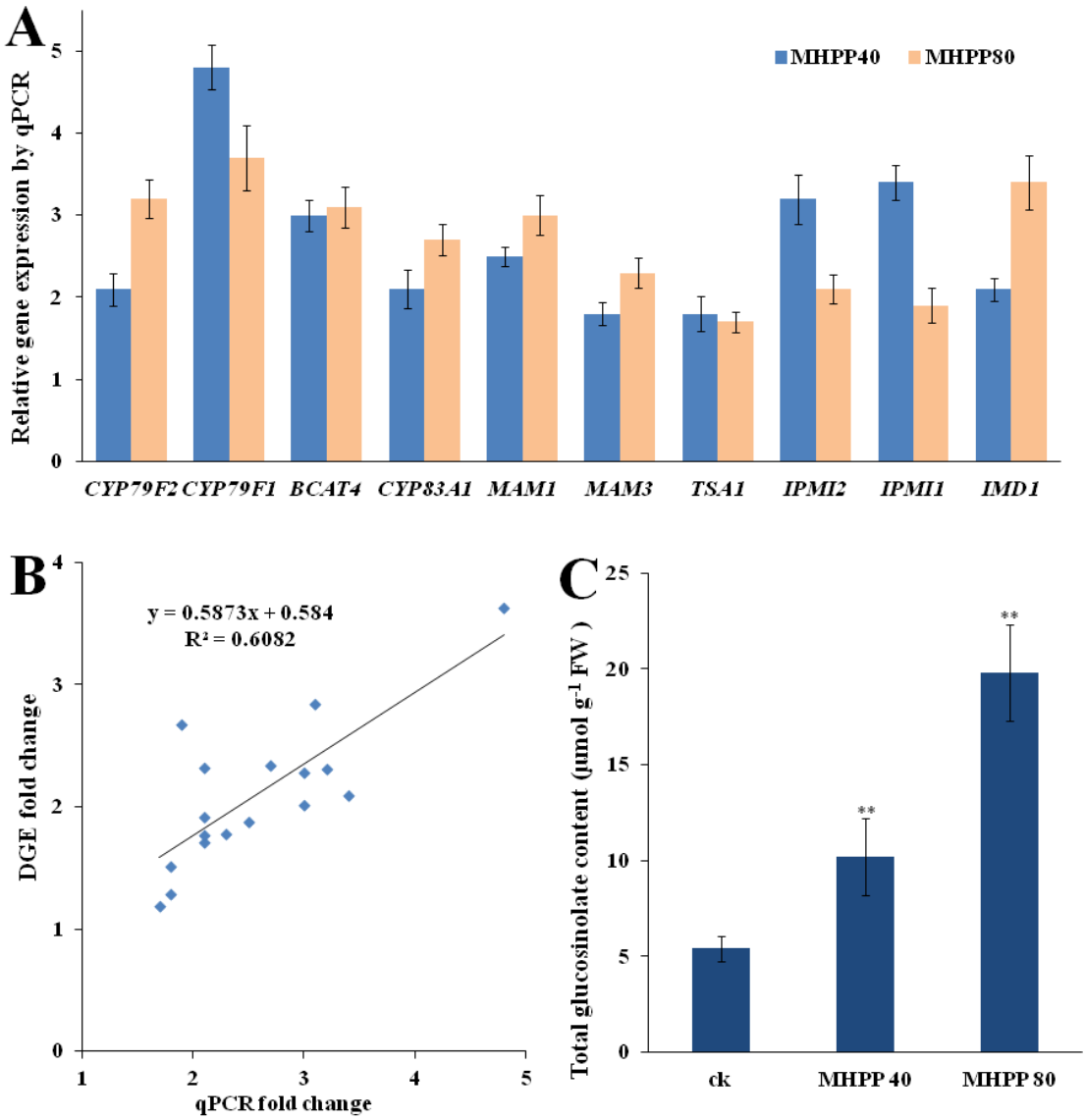

Fig. S16 (A) MHPP up-regulates several genes involved in glucosinolate biosynthesis. Five-day-old wild-type seedlings grown in 1/2 MS medium were treated with 40 μM or 80 μM MHPP for 24 h, and the relative expression levels of 10 glucosinolate biosynthesis-related genes in roots were measured by qRT-PCR. The data are presented relative to those of untreated control seedlings. (B) Reliability analysis of the RNA-seq data based on comparison with the qRT-PCR results. (C) MHPP induces the accumulation of glucosinolates in roots. Five-day-old wild-type seedlings grown in 1/2 MS medium were treated with 40 μM or 80 μM MHPP for 24 h, and the content of the glucosinolates in roots were determined by UPLC-MS/MS. The ± symbol represents the SEM. The asterisks indicate significant differences with respect to the corresponding control based on Tukey's test (**, $P<0.01$).

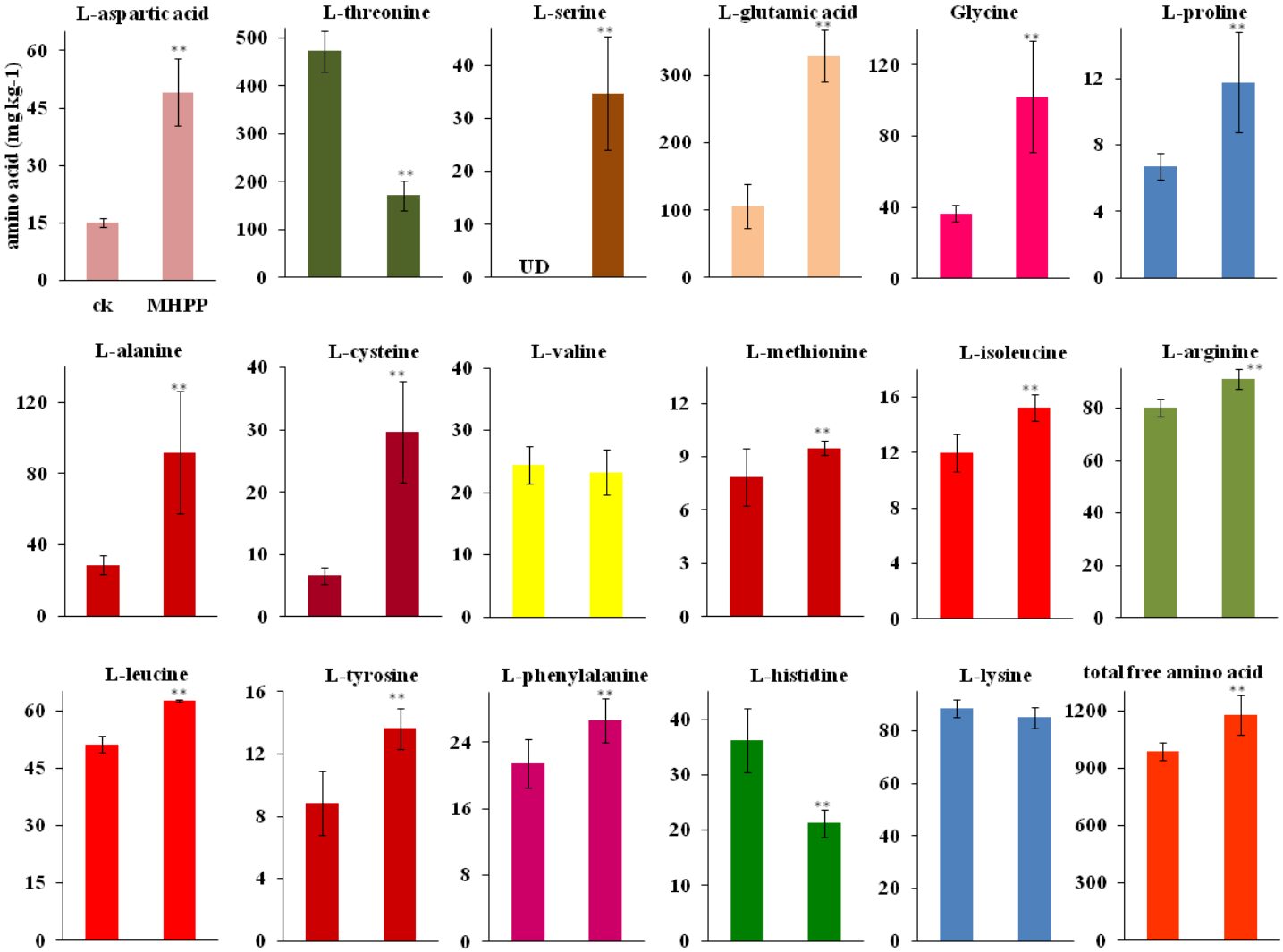

Fig. S17 MHPP affects the free amino acid contents in *Arabidopsis* roots.

Five-day-old wild-type seedlings grown in 1/2 MS medium were treated with 40 μM or 80 μM MHPP for 24 h, and the free amino acid levels in roots were determined by Q-TRAP LC-MS/MS. The ±symbol represents the SEM. The asterisks indicate significant differences with respect to the corresponding control based on Tukey's test (**, P<0.01). UD, undeterminable.

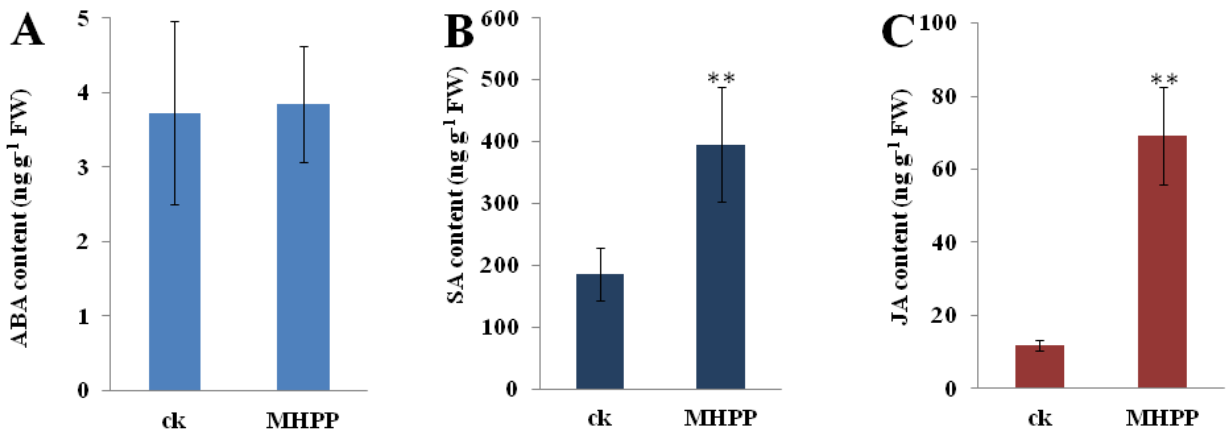

Fig. S18 The contents of ABA, SA, and JA in the roots of wild-type seedlings treated with or without 40 μM MHPP for 24 h. The error bars represent the SEM. The asterisks (**) indicate significant differences with respect to the corresponding control ($P<0.01$ based on Tukey's test).

Supplemental Materials and Methods

Extraction and UPLC-MS/MS Analysis of Glucosinolates

Glucosinolate extraction was performed as described by He et al. (2013). Frozen tissue powder (250 mg) was added to 5 mL of 70% methanol and incubated at 70 ℃ for 20 minutes. After incubation, 1 mL of $Ba(OAc)_2$ (0.4 M) was added, and the sample was centrifuged at 3000 rpm for 5 minutes. Then, the supernatant was added to a DEAE-Sephadex A25 column. The column was then washed twice each with water and 1 mL of sodium acetate (20 mM). Next, sulfatase solution (75 μL) was added to the column, which was left to stand overnight. Desulfonated glucosinolates were eluted in 1 mL aliquots of deionized water and analyzed by UPLC-MS/MS using a Waters ACQUITY UPLC system and a Xevo™ TQ-S mass spectrometer. The samples were separated using an Agilent Zorbax SB-C18 column with a flow rate of 1 mL/min at 30 ℃ as described by Neal (2010) and He et al. (2013). The eluting compounds were monitored at 229 nm. Mass spectral analysis of glucosinolates was performed via positive electrospray ionization (ESI) in multiple reaction monitoring (MRM) mode. The mass spectra of 3-methylsulfinylpropyl (3MSOP), 4-methylsulfinylbutyl (4MSOB), 2-propenyl and 3-butenyl glucosinolates were analyzed based on the detection of individual M_+Na^+ peaks specific for the glucosinolates being tested. The presence of 2-propenyl glucosinolate in the samples was further identified using its standard, which was purchased from Sigma-Aldrich (He et al., 2013).

Amino Acid Quantification by Q-TRAP LC-MS/MS

Frozen tissue powder (100 mg) was added to 500 μL of cold (-20 ℃) metabolite extraction solution (85% (v/v) HPLC-grade methanol, 15% (v/v) MilliQ water, and 100 mg/L ribitol); then, the sample was vortexed and shaken at 1,400 rpm for 20 min at 65 ℃. After a 10 min centrifugation at 15,000 *g*, the supernatant (40 μL) was labeled with iTRAQ reagents (AA 45/32 kit, Applied Biosystems) as recommended by the manufacturer and was analyzed on an Applied Biosystems 3200 Q TRAP LC/MS/MS system that was equipped with an RP-C18 column (150 mm length, 4.6 mm diameter, 5 mm particle size) (Spitzner et al., 2008; Xu et al., 2012).

Visualization of H_2O_2 by the DAB method

For localizing H_2O_2 produced by *Arabidopsis* roots, treated roots were immersed in 1 mg/mL of 3-diaminobenzidine (DAB)-HCl (pH3.8) for 5 h and cleared by boiling in alcohol (95%, v/v) for 5 min. Photos were taken using a Carl Zeiss Imaging System.